




Article

Mineral assemblages and compositional variations in bavenite–bohseite from granitic pegmatites of the Bohemian Massif, Czech Republic

Milan Novák¹, Zdeněk Dolníček^{2*}, Adam Zachař¹, Petr Gadas¹, Miroslav Nepejchal³, Kamil Sobek¹ , Radek Škoda¹ and Luboš Vrtiška²

¹Department of Geological Sciences, Faculty of Science, Masaryk University, Kotlářská 2, CZ-611 37 Brno, Czech Republic; ²Department of Mineralogy and Petrology, National Museum, Cirkusová 1740, CZ-193 00 Prague 9, Czech Republic and ³Retired, Šumperk, Czech Republic

Abstract

The paragenesis and composition of bavenite–bohseite were investigated in fifteen granitic pegmatites from the Bohemian Massif, Czech Republic. Three types distinct in their relation to primary Be precursors, mineral assemblages, morphology and origin were recognised: (1) primary hydrothermal bavenite–bohseite crystallised in miarolitic pockets from residual pegmatite fluids; and secondary bavenite–bohseite in two distinct types: (2) a proximal type restricted spatially to pseudomorphs after a primary Be mineral (beryl > phenakite, helvine–danalite); and (3) a distal type on brittle fractures and fissures of host pegmatite. The mineral assemblages are highly variable: (1) axinite–(Mn), smectite, calcite and pyrite; (2) bertrandite, milarite, secondary beryl, bazzite, K-feldspar, muscovite–illite, scolecite, gismondine–Ca, analcime, chlorite; and (3) muscovite, albite, quartz, epidote, pumpellyite–(Mg), pumpellyite–(Fe³⁺), titanite and chlorite. Electron microprobe analyses showed, in addition to major constituents (Si, Ca and Al), minor concentrations (in apfu) of Na (≤ 0.24), Fe (≤ 0.10), Mn (≤ 0.10) and F (≤ 0.36). The type 1 hydrothermal miarolitic bavenite–bohseite is mostly Al-rich (2.00–0.67 apfu) relative to type 2 proximal bavenite–bohseite and bohseite after beryl, phenakite and helvine–danalite (1.56–0.46, 0.70–0.05, 1.02–0.35 apfu, respectively); and type 3 distal bavenite–bohseite typically after beryl (1.63–0.09 apfu). Raman spectroscopy revealed that the distance between the OH[−] vibrational modes decreases with increasing bohseite component. The Al content of secondary type 2 proximal bavenite–bohseite is controlled by the composition of the Be precursor whereas type 3 distal bavenite–bohseite with beryl as the Be precursor is more variable and the composition is governed mainly by the composition of fluids. Calcium, a crucial component for bavenite–bohseite origins, was derived from residual pegmatite fluids (Vlastějovice, Vepice IV or Třebíč Plutons) or external sources (e.g. Drahonín IV, Věžná I or Maršíkov). Primary type 1 hydrothermal bavenite–bohseite from miarolitic pockets might have crystallised at $T \approx 300$ – 400°C and $P \approx 200$ MPa, whereas the secondary type 2 and 3 bavenite–bohseite formed at $T \approx 300$ – 100°C and $P \approx 200$ – 20 MPa.

Keywords: bavenite, bohseite, mineral assemblages, composition, granitic pegmatite, Bohemian Massif

(Received 8 August 2022; accepted 7 March 2023; Accepted Manuscript published online: 17 March 2023; Associate Editor: Edward Sturgis Grew)

Introduction

Bavenite is a common secondary mineral formed typically after altered beryl in granitic pegmatites, though it is also commonly found as tabular crystals or coatings on crystals of feldspar and quartz in miarolitic pockets with no apparent relation to an altered primary Be mineral (Černý, 2002). An exceptional occurrence has been described from a Ca-skarn (Manning *et al.*, 1983). The composition and crystal structure of bavenite has been discussed in several papers (Hawthorne and Huminicki, 2002; Černý, 2002; Lussier and Hawthorne, 2011 and references therein) demonstrating variable concentrations of Be and Al via the substitution $\text{T}^{(3)}\text{Be} \text{ T}^{(4)}\text{Si} \text{ O}^{(2)}\text{OH} = \text{T}^{(3)}\text{Si} \text{ T}^{(4)}\text{Al} \text{ O}^{(2)}\text{O}$ (Černý, 2002).

Friis *et al.* (2010) originally formulated the bohseite end-member as $\text{Ca}_4\text{Be}_3\text{AlSi}_9\text{O}_{25}(\text{OH})_3$ on the basis of a sample from the Ilímaussaq complex, Greenland. However, subsequent analyses revealed that this formula did not represent the maximum Be content possible, and consequently end-member bohseite was redefined as $\text{Ca}_4\text{Be}_4\text{Si}_9\text{O}_{24}(\text{OH})_4$ (Hålenius *et al.*; 2015; Szeleg *et al.*, 2017).

A very high incompatibility with major and most minor and accessory minerals, with the notable exception of cordierite, sapphirine, staurolite and margarite (Grew *et al.*, 2006) is caused by the relatively small ionic size and low charge of Be^{2+} cations. In addition, the compositional variability of fluids, particularly those associated with granitic pegmatites, results in a diverse suite of Be minerals (Hawthorne and Huminicki, 2002; Grew, 2002; Grew and Hazen, 2014). Because externally imposed chemical potentials govern the stability of Be minerals together with P – T -conditions (e.g. Barton, 1986; Grew, 2002; Wang and Li, 2020), the individual Be minerals and their mineral assemblages can serve as useful geochemical mineral indicators (Burt, 1978;

*Corresponding author: Zdeněk Dolníček; Email: zdenek.dolnicek@nm.cz

Cite this article: Novák M., Dolníček Z., Zachař A., Gadas P., Nepejchal M., Sobek K., Škoda R. and Vrtiška L. (2023) Mineral assemblages and compositional variations in bavenite–bohseite from granitic pegmatites of the Bohemian Massif, Czech Republic. *Mineralogical Magazine* 87, 415–432. <https://doi.org/10.1180/mgm.2023.17>

© The Author(s), 2023. Published by Cambridge University Press on behalf of The Mineralogical Society of the United Kingdom and Ireland. This is an Open Access article, distributed under the terms of the Creative Commons Attribution licence (<http://creativecommons.org/licenses/by/4.0/>), which permits unrestricted re-use, distribution and reproduction, provided the original article is properly cited.

Wood, 1992; Markl and Schumacher, 1997; Markl, 2001; Černý, 2002; Barton and Young, 2002; Franz and Morteani, 2002; Rao *et al.*, 2011; Palinkaš *et al.*, 2014; Uher *et al.*, 2022). Bavenite–bohseite has not been studied experimentally or treated in thermodynamic studies which have been performed solely in the $\text{BeO}-\text{Al}_2\text{O}_3-\text{SiO}_2-\text{H}_2\text{O}$ (BASH) system (e.g. Hsu, 1983; Franz and Morteani, 1984; Barton, 1986) and in the Na–BASH system (Markl, 2001). Černý (2002) assumed an alkaline rather than an acidic environment for the origin of bavenite.

Beryllium minerals are typical accessory phases in the granitic pegmatites classified by Černý and Ercit (2005). Beryl is by far the most abundant primary Be mineral (Černý, 2002; London, 2008; Grew and Hazen, 2014) and only sporadically minor to very rare primary phenakite, chrysoberyl, gadolinite- and helvine-group minerals, rhodizite, londonite, hurlbutite, beryllonite, hambergite (Černý, 2002) and milarite-group minerals (Novák *et al.*, 2017a) also occur in granitic pegmatites. Bavenite–bohseite is one of the most abundant secondary Be minerals in LCT (Li–Cs–Ta) and NYF (Nb–Y–F) pegmatites together with bertrandite and less common milarite-group minerals, bityite, phenakite and several rare species (Černý, 2002; Grew and Hazen, 2014). Bavenite–bohseite also occurs in alkaline pegmatites (Grice *et al.*, 2009; Friis *et al.*, 2010).

We examined textural and paragenetic position, mineral assemblages, composition, and Raman spectra of bavenite–bohseite from a variety of granitic pegmatites in the Bohemian Massif, Czech Republic to determine paragenetic and morphological types, and compositional variability of the bavenite–bohseite series. These were utilised as indicators of fluid composition and mobility of elements (Ca, Be and Al) in hydrothermal conditions, as well as potential sources of fluids. In addition, the mineral assemblages of bavenite–bohseite samples were studied in detail and used below to discuss the stability field of bavenite–bohseite compared to Be minerals in the BASH system.

Brief description of the examined granitic pegmatites

Internal structure

Bavenite–bohseite was examined from granitic pegmatites in various geological regions of the Bohemian Massif, Czech Republic: Moldanubian Zone (11 sites); Silesicum (2 sites); and Lugicum (2 sites) (Fig. 1; Table 1). Intragranitic NYF pegmatite dykes from Vepice IV and several dykes from the Třebíč durbachite pluton (Table 1) evolved from parental melagranite via transitional contacts inwards: a thin granitic unit; a graphic unit; a blocky K-feldspar; and a central miarolitic pocket ($\text{Qz}+\text{Ab}+\text{Kfs}$) developed at the Vepice IV pegmatite. Nests of albite, typically adjacent to quartz core, occur locally in the Třebíč pegmatites. The pegmatites Kracovice, Vlastějovice, Dražice, Drahonín IV and Věžná I (Table 1) exhibit, from the contact inwards, an outer medium-grained granitic unit, a coarse-grained inner unit with abundant graphic intergrowths ($\text{Qz}+\text{Kfs}$, $\text{Qz}+\text{Ab}$, rarely $\text{Qz}+\text{Tur}$, $\text{Qz}+\text{Crd}$), and blocky K-feldspar. Irregular aggregates of albite as well as a well-defined albite unit commonly replace blocky K-feldspar. Miarolitic pockets ($\text{Qz}+\text{Ab}+\text{Kfs}$) occur in Vlastějovice (rare) and Drahonín IV (common) pegmatites. At the Kracovice, Drahonín IV and Věžná I pegmatites, a quartz core is also developed (Table 1). The Ruprechtice pegmatite is known from only a single large fragment of massive quartz from the quartz core and adjacent coarse-grained unit ($\text{Kfs}+\text{Qz}+\text{Ab}+\text{Ms}$). The pegmatite dyke at Nýznerov is composed of a fine-grained border unit, a dominant coarse-grained unit with biotite in the outer portion and muscovite + beryl in the inner portions, and a small quartz core with rare primary phenakite. Two pegmatites from Maršíkov near Šumperk differ in size and degree of tectonic/metamorphic overprint (Table 1). The Schinderhübel I pegmatite forms a thin zoned dyke evolving from a strongly deformed medium-grained wall unit into a coarse-grained intermediate unit locally with saccharoidal albite and ultimately into

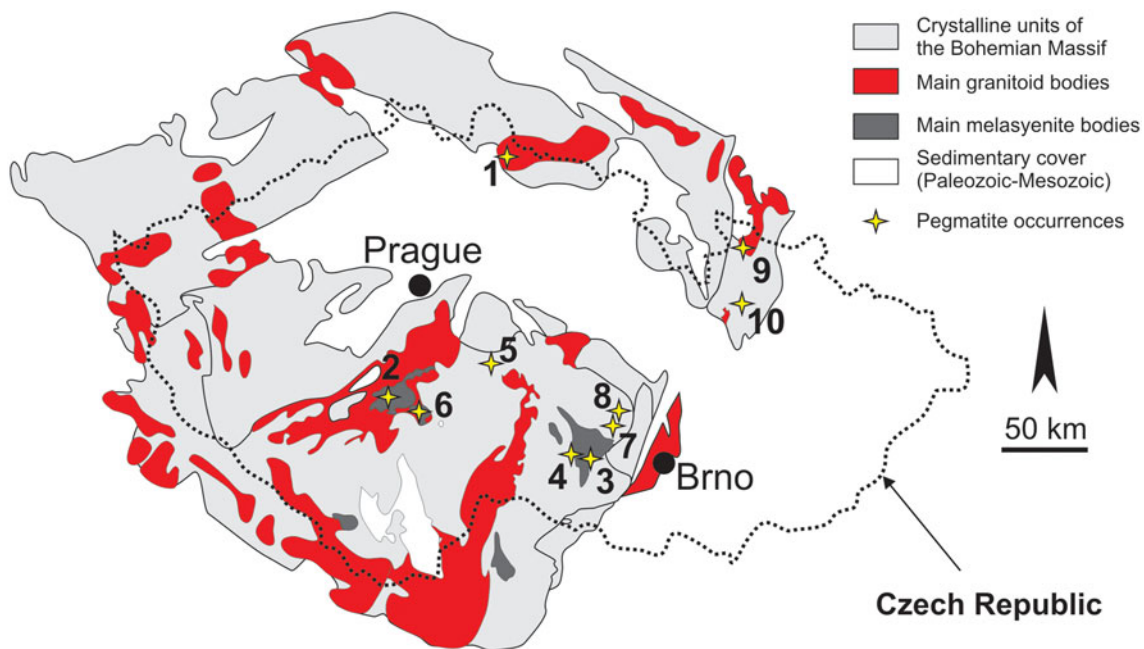


Figure 1. Schematic geological map of the Bohemian Massif with the locations of the investigated pegmatites: 1 – Ruprechtice; 2 – Vepice IV; 3 – Čiměř I and III, Klučov III, Kožichovice I and II; 4 – Kracovice; 5 – Vlastějovice; 6 – Dražice; 7 – Drahonín IV; 8 – Věžná I; 9 – Maršíkov Schinderhübel I, Scheibengraben; and 10 – Nýznerov.

Table 1. Characteristics of the pegmatites investigated.

Family	Type /subtype	Locality	Thickness of dyke in m/host rock	Primary Be minerals (in bold) and typical accessory minerals in a semiquantitative order*	Primary muscovite/ apatite	Pegmatite alterations	Selected subsolidus alterations*	Source**	Sample code
NYF	miarolitic	Ruprechtice	1/l-type Liberec granite	beryl	common/ absent	strong		this work	Rup
NYF	euxenite	Vepice IV	0.3/l-type Milevsko durbachite	Zrn, Py, Clb, Ilm, Rt-Nb, Urn, Cof	absent/rare	weak		this work	Vep
NYF	euxenite	Číměř I	1.2/l-type Třebíč durbachite	helvine > phenakite , Srl, Apy, Ax-Fe, Ax-Mn, Aes-Ce, Eux-Y, Clb, Zrn, Cst, Hzb	absent/very rare	weak	Apy → Pmsd; Cst → Sks; Clb → Fsm, Kse, Ttn, Mic	1	Cima, Cimb
NYF	euxenite	Číměř III	0.5/l-type Třebíč durbachite	phenakite , Drv, Pcl, Clb, Aln-Ce, Act, Zrn	absent/absent	weak	Col → Fsm, Ttn, Dr → Chl	1	Cimc
NYF	euxenite	Klučov III	0.5/l-type Třebíč durbachite	helvine > phenakite , Srl, Cst, Zrn, Clb, Pcl	absent/absent	weak	Cst → Sks	1, 2, 3	Klua, Klub
NYF	euxenite	Kožichovice I	0.3/l-type Třebíč durbachite	beryl , Ilm	absent/absent	weak			Kozb
NYF	euxenite	Kožichovice II	1/l-type Třebíč durbachite	beryl > phenakite , Aes-Ce, Eux-Y, Ttn, Aln-Ce, Drv, Rt-Nb, Py	absent/absent	weak	Ilm → Ttn, Col → Fsm, Kse	1, 2, 3, 4, 5	Koza
Mixed NYF-LCT	lepidolite	Kracovice	1/graphitic gneiss	hambergite, beryl , Srl, Elb, Tpz, Sps, Pln, Fgs-Y, Mnz-Ce	rare/rare	weak		6, 7, 8, 9	Krc
LCT	elbaite	Vlastějovice	2/Fe-skarn	Srl, Elb, Flr, Dbu, Py, Mag, Clb, Cst	absent/rare	weak	Fcpcl → Bi-rich Pcl	10	Vla
LCT	elbaite	Dražice	2/l-type Tábor durbachite	beryl , Srl, Elb, Sps, Lpd, Clb, Cst	absent/absent	strong to weak	dissolved Qz and Tur → Kfs, Non, Ttn	this work	Drza, Drzb
LCT	beryl-columbite	Drahonín IV	1.5/gneiss, amphibolite	beryl , Srl, Sps	absent/rare	strong	Kfs → Ab, Kfs → Ms, Sps → Ms, Chl	11	Draa, Drab
LCT	beryl-columbite	Věžná I	3-4/serpentinite	Be-rich cordierite > beryl , Phl, Drv, Srl, Rt-Nb, Clb, Zrn, Mnz-Ce, Xtm-Y, Elb, Lpd, Trl, Tpz, Pol, Hrm, Cbz-Ca	rare/common	strong	Qz → Krl; Phl → Vrm; Crd → Ms, Chl, Phl, Brl, Prg; Dr, Crd → Ms, Aeg, Arf, Epm, Prg	12, 13, 14, 15, 16, 17, 18, 19, 20	Vez
LCT	beryl-columbite	Nýznerov	2/gneiss	beryl > phenakite , Ap, Clb, Ilm, Alm, Trl, Cst, Rt-Nb, Zrn, Mnz-Ce, Xtm-Y	common/ common	moderate	Clb → Mic, Fsm; Ilm → Ttn, Rt	this work	Nyza, Nyzb
LCT	beryl-columbite	Maršíkov Schinderhübel I	0.5/hornblende gneiss	beryl > chrysoberyl , Sps, Ghn, Clb, Zrn	abundant/rare	moderate	Clb → Fsm, Pcl, Alpine vein - Ep, Pmp, Qz	21, 22, 23	Maa, Mab, Mac
LCT	beryl-columbite	Maršíkov Scheibengraben	10/hornblende gneiss	beryl , Sps, Ghn, Srl, Trl, Tpz, Clb, Mic, Tap-Fe, Zrn	abundant/ common	weak	Kfs → Ab, Kfs → Ms, Clb → Fsm, Mic	24	Mae

* Symbols according to Warr (2021).

** Sources: 1 – Zachař *et al.* (2020); 2 – Škoda *et al.* (2006); 3 – Novák *et al.* (2011); 4 – Novák and Filip (2010); 5 – Výravský *et al.* (2019); 6 – Němec (1990); 7 – Čopjaková *et al.* (2015); 8 – Novák *et al.* (2012); 9 – Novák *et al.* (1998); 10 – Novák *et al.* (2013); 11 – Sojka (1969); 12 – Černý (1960); 13 – Černý (1963); 14 – Černý (1965); 15 – Novák *et al.* (2015b); 16 – Dosbaba and Novák (2012); 17 – Toman and Novák (2018); 18 – Toman and Novák (2020); 19 – Gadas *et al.* (2020); 20 – Čopjaková *et al.* (2021); 21 – Černý *et al.* (1992); 22 – Chládek *et al.* (2021); 23 – Dolníček *et al.* (2020); and 24 – Novák *et al.* (2003).

a small quartz core (Černý *et al.*, 1992; Chládek *et al.*, 2020, 2021). In the Scheibengraben pegmatite dyke, up to ~10 m thick, individual pegmatite units (coarse-grained, graphic, blocky K-feldspar) are rather irregularly distributed; late saccharoidal albite extensively replaced the other pegmatite units (Novák *et al.*, 2003) and the tectonic overprint is weak to moderate.

Primary Be minerals, their mineral assemblages and compositions

Primary Be minerals as precursors of secondary bavenite–bohseite have been described from numerous localities (e.g. Třebíč Pluton – Zachař, 2021). At the Třebíč euxenite-type pegmatites, two distinct assemblages of primary Be minerals were recognised by Zachař *et al.* (2020); the assemblage B (beryl ± phenakite) and the assemblage HD (helvine–danalite ± phenakite). Beryl and helvine–danalite typically do not occur within the same pegmatite body (Table 1). Beryl forms prismatic greenish crystals, up to 5 cm in length, in albite and quartz (Novák and Filip, 2010; Zachař *et al.*, 2020). Strongly-altered equidimensional grains to subhedral crystals of reddish brown (fresh) to dark brown (altered) helvine–danalite, up to 5 cm in size, occur in tourmaline-bearing pegmatites from a graphic unit, a blocky unit, and albite-rich portions. Rare prismatic colourless crystals of phenakite, up to 3 cm in length, typically from massive quartz, are usually fresh (Zachař *et al.*, 2020). No primary Be mineral has been identified at the Vlastějovice (Novák *et al.*, 2013) and Vepice IV pegmatites. Beryl is the sole primary Be mineral at the Dražice, Drahonín IV, Ruprechtice and Scheibengraben pegmatites (Table 1). Rare hambergite (Němec, 1990; Novák *et al.*, 1998), chrysoberyl (Černý *et al.*, 1992) and phenakite were identified together with dominant beryl in the Kracovice, Schinderhübel I and Nýznerov pegmatites, respectively; however, typically these minerals were not altered (Table 1). Phenakite and hambergite are evidently primary minerals, whereas chrysoberyl is a product

of tectono-metamorphic overprinting (Černý *et al.*, 1992). Beryl forms short to long prismatic subhedral to euhedral crystals, 1–10 cm in diameter. Secondary pockets formed from dissolved prismatic crystals of beryl at the Drahonín IV pegmatite were up to ~40 cm in length (Sojka, 1969). A radial aggregate of strongly altered beryl from Ruprechtice, up to ~10 cm in diameter, is located at the contact of massive quartz and a coarse-grained unit. Beryl- and Be-enriched cordierite occur in the Věžná I pegmatite (Table 1). Less commonly beryl forms greyish prismatic crystals, up to 20 cm in length, typically strongly altered. Primary Be minerals at all examined localities are enclosed mostly in albite, in albitised K-feldspar, or in massive quartz of the quartz core typically adjacent to an albite-rich unit.

Representative compositions of primary beryl and helvine–danalite from some localities are given in Tables 2 and 3. Contents of Na, Mg and Fe are relatively elevated in beryl from pegmatites of the Třebíč Pluton and in Nýznerov, whereas beryl from Kracovice and Dražice pegmatites is close to the ideal composition, or is only slightly enriched in Na. Compositions of helvine–danalite are close to the midpoint between both end-members with negligible Zn contents. Phenakite compositions are very close to the ideal formula (Zachař *et al.*, 2020).

Samples and analytical methods

The samples of bavenite–bohseite were obtained from several sources including the mineralogical collections of the Moravian Museum, Brno (8) and the National Museum, Prague (4), and the research collections of A. Zachař (5), M. Nepejchal (2) and M. Novák (2). The abbreviations for the minerals used in the text and figures are after Warr (2021).

Analyses of the samples were performed using Cameca SX-100 electron microprobes operating in the wavelength-dispersive (WDS) mode at the National Museum, Prague (1), and the

Table 2. Representative compositions of primary beryl (see Table 1 for sample codes).

Sample	Rup	Kozb	Koza	Krc	Drza	Drab	Nyzb	Maa
Wt.%								
SiO ₂	67.74	64.92	65.40	66.71	66.98	68.69	65.51	68.26
Al ₂ O ₃	18.64	14.63	14.34	18.91	19.10	18.50	13.74	18.88
Sc ₂ O ₃	n.d.	0.20	0.15	b.d.l.	b.d.l.	0.02	b.d.l.	b.d.l.
BeO	14.15	13.43	13.47	13.90	13.99	14.21	13.57	14.19
MgO	0.08	2.17	2.15	b.d.l.	b.d.l.	b.d.l.	2.30	b.d.l.
FeO	0.88	0.54	0.75	0.08	0.09	0.30	2.05	0.43
ZnO	0.10	n.d.	n.d.	n.d.	n.d.	0.38	0.11	b.d.l.
Na ₂ O	0.31	1.73	1.59	0.12	0.15	0.12	1.91	0.19
K ₂ O	b.d.l.	0.14	0.25	b.d.l.	b.d.l.	b.d.l.	b.d.l.	b.d.l.
Cs ₂ O	0.07	0.08	0.23	0.14	0.07	n.d.	b.d.l.	n.d.
Total	102.04	97.86	98.37	99.88	100.43	101.89	99.23	102.05
Apfu*								
Si ⁴⁺	5.977	6.036	6.065	5.992	5.980	6.034	6.029	6.006
Al ³⁺	1.939	1.604	1.568	2.002	2.010	1.916	1.491	1.958
Sc ³⁺		0.016	0.012	0.000	0.000	0.001		0.000
Be ²⁺	3.000	3.000	3.000	3.000	3.000	3.000	3.000	3.000
Mg ²⁺	0.011	0.301	0.297	0.001	0.001	0.001	0.315	0.001
Fe ²⁺	0.065	0.042	0.058	0.006	0.007	0.022	0.157	0.032
Zn ²⁺	0.007					0.025	0.008	
Na ⁺	0.053	0.312	0.286	0.021	0.026	0.021	0.341	0.032
K ⁺		0.017	0.030					
Cs ⁺	0.003	0.003	0.009	0.005	0.003			
Σcations	11.060	11.333	11.328	11.028	11.031	10.999	11.344	11.036

*The formulae were calculated on the basis of T + M = 8 apfu and stoichiometric Be = 3 apfu.
b.d.l. – below detection limit; n.d. – not detected

Table 3. Representative compositions of primary helvine–danalite (see Table 1 for sample codes).

Sample	Cima	Cima	Cima	Klub
Wt. %				
SiO ₂	33.41	33.45	33.50	32.43
BeO	13.90	13.92	13.94	13.50
MgO	0.09	b.d.l.	b.d.l.	b.d.l.
MnO	18.55	24.59	29.46	23.51
FeO	28.65	24.63	19.68	26.22
ZnO	4.07	1.51	1.84	1.68
S	5.09	5.11	5.31	5.65
O=S	-2.54	-2.55	-2.65	-2.82
Total	101.21	100.65	101.08	100.16
Apfu*				
Si ⁴⁺	3.000	3.000	3.000	3.000
Be ²⁺	3.000	3.000	3.000	3.000
Mg ²⁺	0.012			
Mn ²⁺	1.411	1.868	2.235	1.842
Fe ²⁺	2.152	1.847	1.474	2.029
Zn ²⁺	0.270	0.100	0.121	0.114
Σcations	9.844	9.816	9.830	9.985
S ²⁻	0.856	0.859	0.890	0.979
O ²⁻	11.988	11.957	11.940	12.006

*The formulae were calculated on the basis of Si = 3 apfu and stoichiometric Be = 3 apfu. b.d.l. – below detection limit.

Department of Geological Sciences, Masaryk University Brno, Czech Republic (2). Bavenite–bohseite was analysed using an acceleration voltage of 15 kV, beam current of 10 nA (1) or 15 nA (2), and 2–5 μm beam diameter (1, 2). The following analytical lines and standards were used: apatite (PKα); wollastonite (SiKα, CaKα); sanidine (AlKα); (1) hematite or (2) andradite (FeKα); (1) diopside or (2) Mg₂SiO₄ (MgKα); (1) rhodonite or (2) spessartine (MnKα); albite (NaKα); (1) LiF or (2) topaz (FKα); and halite (ClKα). The peak counting times were usually between 20 and 30 s, those of both backgrounds were between 10 and 15 s. Raw intensities were converted to the concentrations of oxides using the automatic ‘PAP’ matrix-correction procedure (Pouchou and Pichoir, 1985), including model calculation of BeO to the analytical sum of 100 wt.% and correction of overlaps for P/Ca and Rb/Si. Contents of other elements measured, which are not included in the tables (Ti, Sb, V, Cr, Pb, Zn, Ba, Sr, Cu, Co, Ni, Cs, Rb, K and N), were analysed quantitatively, however the values were below the detection limit (0.04–0.08 wt.% for most elements). Calculation of empirical formula in atoms per formula unit (apfu) was modified according to Lussier and Hawthorne (2011) and Szełęg *et al.* (2017) due to the presence of additional minor cations. The calculation was normalised to a sum of 13 cations except for Na and Ca. The Be content was then iterated until Na+Ca = Al+Be+Mg+Fe+Mn. The water content is based on charge balance, assuming 28 anions. The mol.% of the bavenite component was calculated from the ^{ivb}Al value, which is total Al (apfu) minus ^{iva}Al, the latter substituting for Si (assuming Si+^{iva}Al = 9 apfu).

Raman spectra of all the samples were obtained with a LabRam HR Evolution Raman spectrometer system by HORIBA (Horiba Jobin Yvon) with a Peltier-cooled CCD detector and Olympus BX-41 microscope at room temperature, at the Department of Geological Sciences, Masaryk University, Brno. Spectra were calibrated using the Rayleigh line with the 532 nm emission of a Nd:YAG laser. Excitations at 473 nm and 633 nm were chosen to verify the measurements and to eliminate possible analytical artefacts caused by laser-induced photoluminescence. We have

recorded the full Raman spectra by scanning the entire range of interest 100–4000 cm⁻¹ using a diffraction grating with 600 grooves per mm, an entrance slit of 100 μm, a confocal hole at 200 μm or 100 μm and a 50× objective lens. The diameter of the spot for the measurement is ~1 μm. Acquisition time was set to 20 or 40 s and four accumulations. Data were processed with Seasolve *PeakFit 4.1.12* and *LabSpec 6* software. Band fitting was done after appropriate background correction, assuming Lorentzian–Gaussian band shapes.

Results

Textures and mineral assemblages

We recognised several types of bavenite–bohseite distinct in their relation to an obvious or potential primary Be precursors, overall mineral assemblage and morphology (Table 4): type 1 primary hydrothermal bavenite–bohseite from miarolitic pockets; and two types of secondary bavenite–bohseite i.e. – type 2 proximal in pseudomorphs after a primary Be mineral and type 3 distal on brittle tectonic fractures and fissures of a host pegmatite generally close to altered beryl (Figs 2, 3; see also Novák *et al.*, 2015a).

Radial aggregates of tabular or fibrous crystals of bavenite, up to 1.5 cm in size, overgrowing crystals of primary K-feldspar, albite, or quartz in miarolitic pockets, up to 5 cm in size, from the Vlastějovice and Vepice IV pegmatites represent the hydrothermal miarolitic type. The hydrothermal minerals associated with bavenite–bohseite in miarolitic pockets include, at Vlastějovice, zoned, Sn-enriched (≤4.67 wt.% SnO₂) axinite-(Mn) + late smectite (Fig. 3a), and at Vepice IV, abundant calcite + pyrite (Table 4).

Proximal secondary Be minerals directly replacing a primary Be mineral in pseudomorphs are typical in pegmatites of the Třebíč Pluton (Table 4; Fig. 2a–e). Bavenite–bohseite in thin veinlets cutting primary Be minerals and as rare masses in helvine–danalite, is the most widespread mineral and predominates over minor to rare milarite, agakhanovite, bazzite, secondary beryl, secondary phenakite, secondary danalite, bertrandite and gismondine-Ca (Table 4; see also Novák and Filip, 2010; Zachař *et al.*, 2020). Rare chalk-like coatings of secondary bavenite–bohseite also are developed on the surface of crystals or very close (<~1–2 mm) to the crystals of altered beryl (Fig. 2d; Kožichovice II – Novák and Filip, 2010; Zachař *et al.*, 2020). Typical distal fissure-filling assemblages of secondary Be minerals developed on brittle tectonic fractures and fissures have not been found in this pegmatite region.

The following pegmatites contain only proximal bavenite–bohseite. At Ruprechtice, radial aggregates after beryl consist of proximal white bavenite–bohseite and colourless crystals of bertrandite in a mass of dominant secondary fine-grained greenish muscovite–illite + K-feldspar, and rare zeunerite. Bavenite–bohseite and bertrandite are not associated spatially and beryl is present in large relics. At the Kracovice pegmatite, rare grains of beryl are replaced by radial aggregates of bavenite + euhedral bertrandite; rare aggregates of K-feldspar and gismondine-Ca are enclosed in bavenite (Fig. 2f). At the Drahonín IV pegmatite, two distinct proximal secondary bavenite–bohseite assemblages were recognised: (1) rare bavenite–bohseite + euhedral bertrandite in thin veinlets replacing beryl are associated typically with abundant analcime, rare scolecite, laumontite and gismondine-Ca (Fig. 3b), and very rare fluorapatite + chlorite (Table 4); (2) abundant massive aggregates of bavenite–bohseite

Table 4. Mineral assemblages of bavenite–bohseite.

Position/ sample	Be mineral(s)				Associated hydrothermal or secondary minerals
	Replaced/altered primary magmatic	Hydrothermal in miarolitic pocket	Secondary – proximal	Secondary – distal	
Rup	beryl		bohseite > bavenite, bertrandite		muscovite–illite, zeunerite
Vep	absent	bavenite >> bohseite			calcite, pyrite
Cima	helvine		bohseite > bavenite		
Klub	helvine		bohseite >> bavenite		
Klua	phenakite		bohseite, milarite		
Cimb	phenakite		bohseite		
Cimc	phenakite		bohseite		titanite
Kozb	beryl		bohseite > bavenite, milarite		
Koza	beryl		bohseite > bavenite, beryl, milarite, bazzite		smectite, gismondine-Ca
Krc	beryl		bavenite, bertrandite		adularia, gismondine-Ca
Vla	absent	bavenite			axinite-(Mn), smectite
Drza	beryl		bavenite		
Drzb	beryl			bavenite > bohseite, milarite	adularia
Draa	beryl		bohseite > bavenite, bertrandite		analclime, scolecite, pyrite, gismondine-Ca
Drab	beryl		bohseite > bavenite, bertrandite		chlorite, fluorapatite, sphalerite
Vež	beryl, Be-rich cordierite			bohseite	titanite, chlorite
Nyza	beryl		bohseite > bavenite		titanite
Nyzb	beryl			bavenite > bohseite	
Maa	beryl		bohseite > bavenite		
Mab	beryl			bohseite > bavenite	albite, muscovite, quartz
Mac	beryl			bohseite > bavenite	epidote, pumpellyite-(Mg), pumpellyite-(Fe ³⁺), quartz
Mae	beryl			bohseite	

with euhedral crystals of bertrandite occur in secondary pockets after almost completely dissolved large crystals of beryl (Fig. 3c). Beryl is almost exclusively directly replaced by bavenite–bohseite (Kracovice, Drahonín IV) (Figs 2f, 3b) and bertrandite was only found exceptionally in a direct contact with the replaced beryl.

At the pegmatite outcrops from Dražice, beryl is mostly fresh. It is strongly altered or replaced completely by proximal bavenite–bohseite only if the beryl crystal is cut by or located close (<~5 cm) to brittle tectonic fractures which continue to the host rock. Distal bavenite is developed exclusively on such fractures and is associated with abundant late K-feldspar (adularia). Proximal bavenite–bohseite replaces beryl, whereas euhedral crystals of bertrandite are enclosed in a bavenite matrix. Very rare milarite was found in a small vug close to a distal bavenite + K-feldspar aggregate. In the Věžná I pegmatite, rare crystals and aggregates, <2 mm in size, and fine-grained coatings of bohseite are associated with titanite and chlorite on fractures of blocky K-feldspar + quartz and have no apparent relationship to a possible primary Be-rich precursor (see also Černý, 1965).

Rare radial and chalk-like aggregates of proximal bavenite–bohseite are developed after altered crystals of beryl, relics of which are abundant in the Nýznerov pegmatite (Table 4). Volumetrically dominant bavenite–bohseite was observed only locally in the assemblage bertrandite + K-feldspar ± chlorite. In the Maršíkov pegmatites, proximal bavenite–bohseite in pseudomorphs after beryl was found at the Schinderhübel I pegmatite (Fig. 3d). Radial aggregates of chalky white distal bavenite–bohseite on tectonic fractures apparently not associated with other secondary minerals is the most common type (Table 4). They commonly occur between large flakes of primary muscovite at

the Schinderhübel I pegmatite (Fig. 3f), whereas the textural relations of bavenite–bohseite with associated albite, muscovite and quartz on fractures are not clear. They are probably fragments of the fracture surface where late bavenite–bohseite crystallised (see also Dolníček *et al.*, 2020); however, the euhedral habit of quartz grains (see Fig. 3e) indicates that it recrystallised during or slightly before the formation of bavenite–bohseite. Only scarcely, is bavenite–bohseite associated closely with Sr-enriched epidote (≤1.75 wt.% SrO) + F-enriched (≤0.45 wt.% F) pumpellyite-(Mg) to pumpellyite-(Fe³⁺) on Alpine-type hydrothermal veins, ~3 mm thick, cutting a small quartz core at the Schinderhübel I pegmatite (Fig. 3e). Bavenite–bohseite is developed mostly at the external part of the breccia as a matrix of euhedral grains of recrystallised quartz (Fig. 3e) coeval with epidote and pumpellyite.

We also explored the abundance of primary muscovite in the pegmatites as an indicator of the peraluminous nature and acidic conditions in granitic pegmatites (e.g. London, 2008). Primary muscovite is absent in all NYF pegmatites, both elbaite-subtype pegmatites Dražice and Vlastějovice, and it is rare at the Věžná I and Kracovice pegmatites (Table 1). In contrast, it is very abundant at the pegmatites from Maršíkov and it is associated locally with distal bavenite–bohseite (Fig. 3f; Table 4). Primary muscovite is common at Ruprechtice and Nýznerov. Further, the abundance of fluorapatite, a sink for Ca in late stages of pegmatite evolution (Martin and de Vito, 2014), was investigated. Primary apatite is mostly absent in NYF pegmatites and very rare in a majority of the examined LCT pegmatites; it is common only at the Nýznerov, Věžná I and Scheibengraben pegmatites (Table 1). Very rare, thin veinlets of late fluorapatite associated with proximal bavenite–bohseite + bertrandite were found in the Drahonín IV and Dražice pegmatites (Table 4).

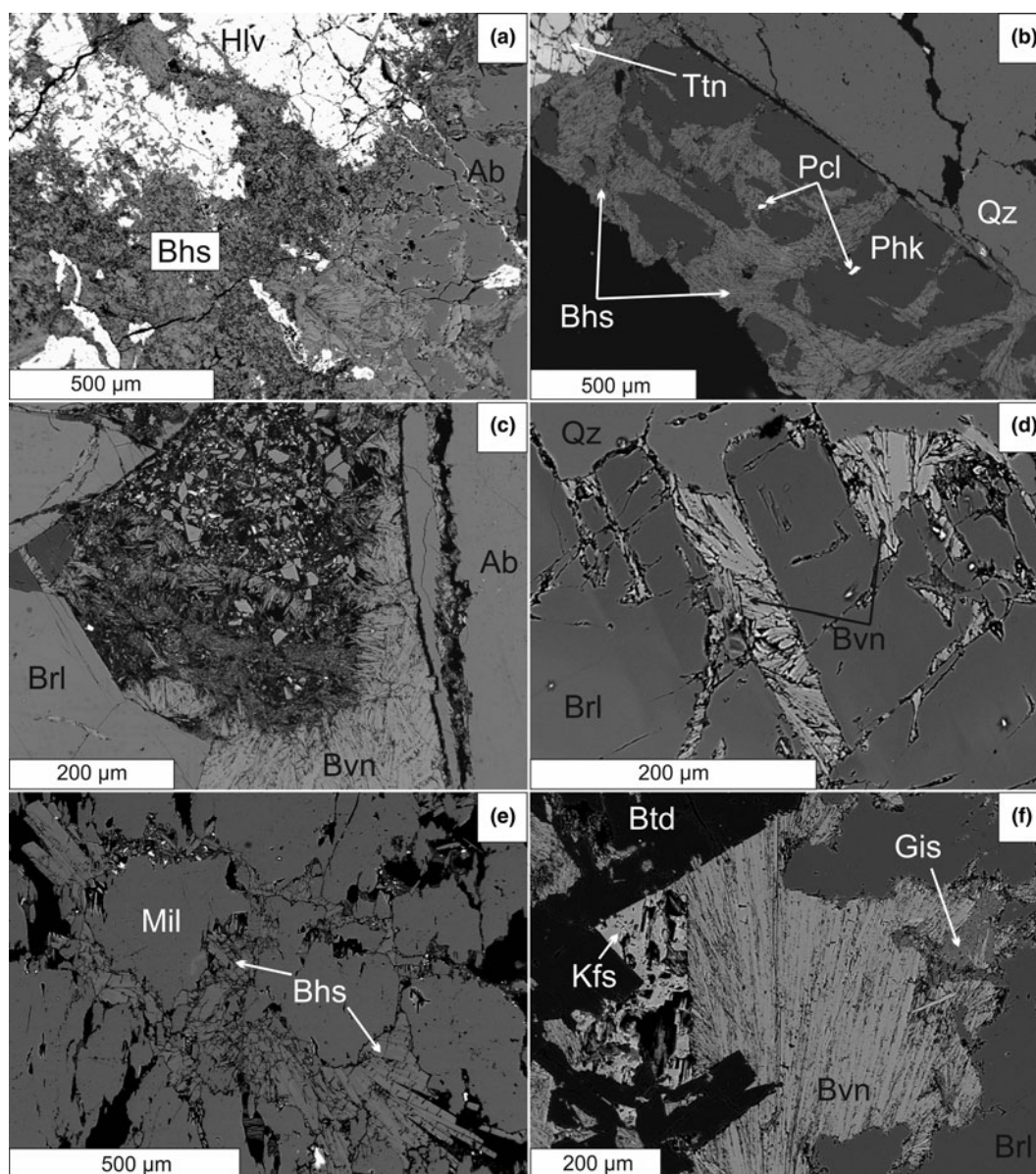


Figure 2. BSE images of primary and secondary Be minerals from pegmatites of the Třebíč Pluton. (a) Helvite enclosed in albite replaced by a fine-grained aggregate of proximal bohseite from Číměř I. (b) Phenakite replaced by proximal bohseite, note inclusions of pyrochlore, Číměř III. (c) and (d) Proximal and ‘near-distal’ bavenite–bohseite overgrowing and replacing zoned beryl, Kožichovice II. (e) Secondary proximal milarite and bohseite after helvite, Číměř I. (f) Complex proximal secondary assemblage after beryl with common bavenite–bohseite, bertrandite, K-feldspar and rare gismondine, Kracovice.

Composition of bavenite–bohseite

Compositions were obtained using electron probe micro-analyses (EPMA), hence, the contents of Be and H₂O were calculated from stoichiometry according to the modified procedure of Lussier and Hawthorne (2011). The measured concentrations of Al are critical for the discussion, whereas Na, Fe, Mn, P and F are of secondary importance as only trace amounts are usually present (Table 5). Data obtained during our study and from the published papers of Novák and Filip (2010), Dolníček *et al.* (2020) and Zachař *et al.* (2020) revealed high variability in Al (and Be) and significant heterogeneity of some samples (Fig. 4). Unfortunately, the similar atomic numbers of the elements in bavenite–bohseite minerals make standard back-scattered electron (BSE) images less useful for the study of zoned structures of bavenite–bohseite crystals.

Two samples of type 1, hydrothermal bavenite and bavenite–bohseite from miarolitic pockets, yielded the highest Al concentrations (all data in this paragraph given in apfu) – Vlastějovice (2.00–1.12) and Vepice IV (2.00–0.67) (Fig. 4). Type 2 proximal bavenite–bohseite is more variable in Al concentrations (1.56–0.05). Solid solutions with dominant bohseite having very low to moderate Al (1.02–0.05) are typical in the pseudomorphs after Al-free precursors phenakite and helvite–danalite whereas in the beryl pseudomorphs bavenite–bohseite has higher Al (1.56–0.69). Type 3, distal bavenite–bohseite, yielded high variability in Al contents (1.63–0.09). Elevated Al (1.63–0.58) is typical for the Schinderhübel I pegmatite associated with muscovite and for bavenite–bohseite from Dražice (1.63–0.96) whereas bohseite from Věžná I is Al-poor (0.34–0.09).

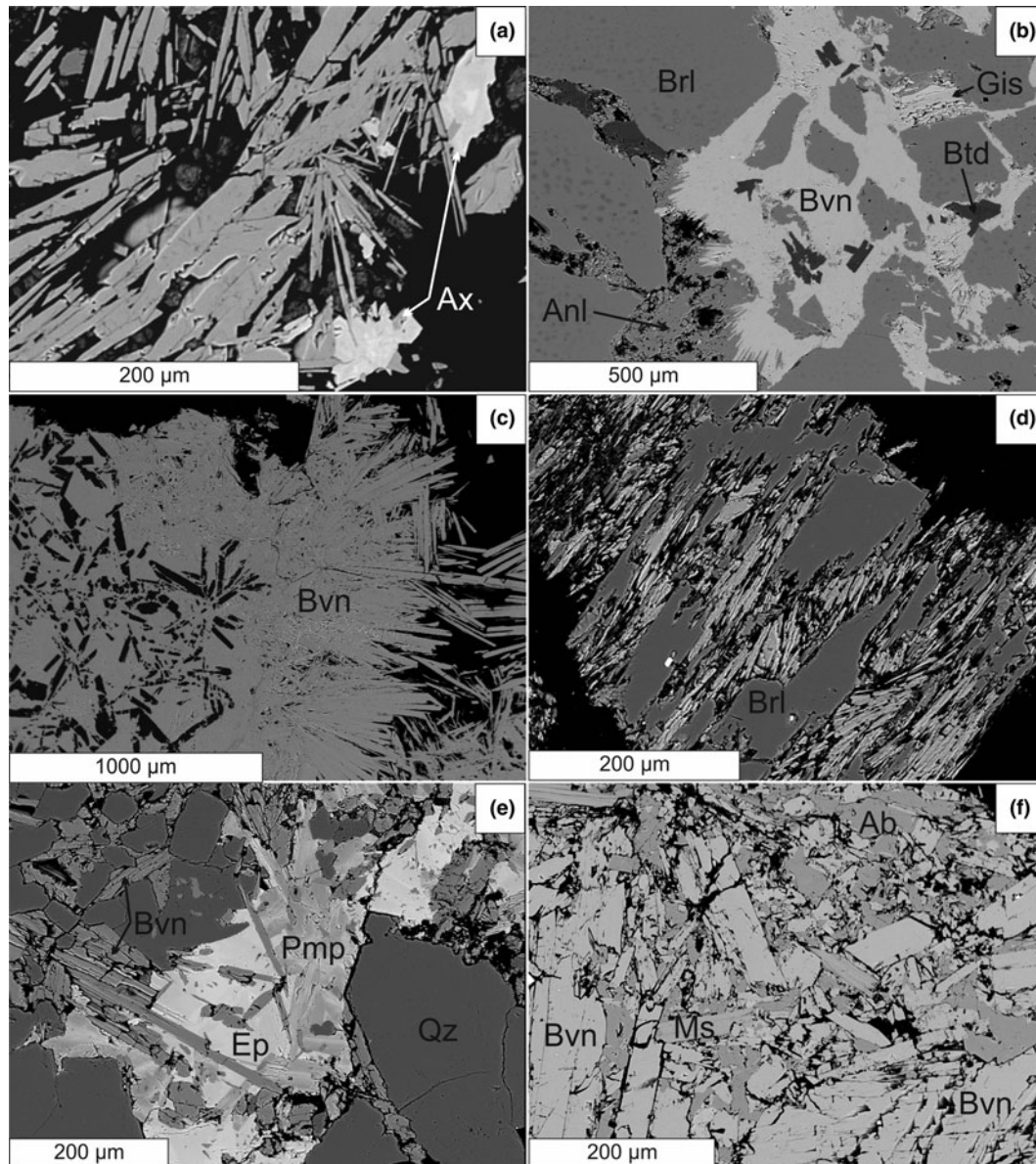


Figure 3. BSE images of primary and secondary Be minerals from the pegmatites Vlastějovice, Drahonín and Maršíkov Schinderhübel I. (a) Hydrothermal bavenite from a miarolitic pocket associated with heterogeneous grains of axinite-Mn from Vlastějovice. (b) Beryl replaced by proximal bavenite-bohseite with small euhedral grains of bertrandite, gismondine and analcime, Drahonín IV. (c) Aggregate of proximal bavenite-bohseite with euhedral crystals of bertrandite, Drahonín IV. (d) Proximal bavenite-bohseite after beryl, Maršíkov Schinderhübel I. (e) Distal bavenite-bohseite in fracture from massive quartz, note associated epidote and pumellyite and euhedral quartz, Maršíkov Schinderhübel I. (f) Distal bavenite-bohseite associated with muscovite and albite, Maršíkov Schinderhübel I.

We also focused our study on minor to trace elements, which have not been reported in the majority of the literature cited. Low concentrations of Na (~ 0.2 wt.% Na_2O) are typical in most data (Table 5); however, higher concentrations were found in the distal bohseite from Věžná I (≤ 0.71 wt.% Na_2O ; ≤ 0.20 apfu Na). Proximal bavenite-bohseite from the Třebíč pegmatites also contains minor concentrations of Fe (≤ 0.59 wt.% FeO, ≤ 0.07 apfu Fe) in bavenite-bohseite after beryl (Kožichovice I) and in bohseite after helvine-danalite from Čiměř I (≤ 0.74 wt.% FeO, ≤ 0.10 apfu Fe) and Mn (≤ 0.81 wt.% MnO, ≤ 0.10 apfu Mn) in the latter. Concentrations of P close to the detection limit were obtained in the Věžná I (≤ 0.10 apfu P) and Maršíkov Schinderhübel I (≤ 0.13 apfu P) pegmatites. Concentrations of F are mostly low (≤ 0.2 wt.% F); the highest concentration

(≤ 0.74 wt.% F) was found in the proximal bavenite-bohseite from the Nýznerov pegmatite.

The zoned composition of a single crystal within a radial aggregate was examined at several localities where samples suitable for such study were available. Zoning was found in the hydrothermal miarolitic bavenite from Vlastějovice; from 1.30 apfu Al in the base to 1.96 apfu Al in the top of a single platelet. In contrast, at the Ruprechtice and Nýznerov pegmatites, single platelets are almost homogeneous, and no apparent compositional evolution was observed. Hence, the individual crystals of bavenite-bohseite vary from almost homogeneous to highly heterogeneous. The highest variability within the examined sample (several fragments were studied) was observed for the hydrothermal bavenite-bohseite from the miarolitic pocket at Vepice IV

Table 5. Representative compositions of bavenite–bohseite.

An. No. Sample Type	1 Rup Brl	2 Rup Brl	3 Cima Hlv	4 Klub Hlv	5 Klua Phk	6 Cimb Phk	7 Cimc Phk	8 Kozb Brl	9 Koza Brl	10 Koza Brl	11 Krc Brl	12 Krc Brl
Wt.%												
SiO ₂	59.24	58.67	59.63	59.79	58.88	59.48	59.73	58.24	58.56	58.26	58.30	59.59
Al ₂ O ₃	6.22	4.95	4.54	4.20	0.85	2.50	5.06	6.22	4.31	5.86	8.54	5.95
BeO*	7.86	8.36	8.34	8.20	10.86	9.82	8.43	7.73	8.73	8.07	6.77	8.05
MnO	b.d.l.	b.d.l.	0.81	0.39	0.11	b.d.l.	b.d.l.	b.d.l.	0.08	b.d.l.	b.d.l.	0.09
FeO	b.d.l.	b.d.l.	0.31	0.32	b.d.l.	b.d.l.	b.d.l.	0.32	0.09	b.d.l.	b.d.l.	b.d.l.
CaO	23.90	23.91	24.13	23.02	25.16	24.58	24.16	24.43	23.94	24.41	24.30	24.34
Na ₂ O	0.31	0.15	0.25	0.30	0.12	0.11	0.17	b.d.l.	0.28	0.07	0.16	0.18
H ₂ O*	2.93	2.96	3.15	3.17	3.60	3.45	3.00	2.69	3.13	2.89	2.36	2.87
F	b.d.l.	0.23	0.18	0.19	0.54	0.22	0.26	0.22	0.21	b.d.l.	0.18	0.22
O=F	0.00	-0.10	-0.08	-0.08	-0.23	-0.09	-0.11	-0.09	-0.09	0.00	-0.08	-0.09
Total	100.46	99.13	101.25	99.51	99.90	100.07	100.69	99.75	99.23	99.56	100.52	101.19
Atoms per formula unit												
Si ⁴⁺	9.013	9.017	9.018	9.140	8.894	8.988	9.035	8.969	8.982	8.958	8.955	9.005
^{iva} Al ³⁺	0.000	0.000	0.000	0.000	0.106	0.012	0.000	0.031	0.018	0.042	0.045	0.000
Subtotal	9.013	9.017	9.018	9.140	9.000	9.000	9.035	9.000	9.000	9.000	9.000	9.005
^{ivb} Al ³⁺	1.115	0.897	0.809	0.757	0.045	0.434	0.903	1.099	0.762	1.019	1.501	1.060
Be ²⁺	2.872	3.086	3.031	3.012	3.941	3.566	3.062	2.861	3.216	2.981	2.499	2.924
Mn ²⁺	b.d.l.	b.d.l.	0.103	0.051	0.015	b.d.l.	b.d.l.	b.d.l.	0.011	b.d.l.	b.d.l.	0.011
Fe ²⁺	b.d.l.	b.d.l.	0.039	0.040	b.d.l.	b.d.l.	b.d.l.	0.041	0.011	b.d.l.	b.d.l.	b.d.l.
Subtotal	3.987	3.983	3.982	3.860	4.000	4.000	3.965	4.000	4.000	4.000	4.000	3.995
Ca ²⁺	3.896	3.938	3.910	3.771	4.072	3.980	3.915	4.032	3.935	4.021	3.998	3.941
Na ⁺	0.091	0.045	0.072	0.089	0.035	0.033	0.050	b.d.l.	0.083	0.021	0.047	0.053
Subtotal	3.987	3.982	3.982	3.861	4.107	4.012	3.965	4.032	4.017	4.042	4.045	3.994
H ⁺	2.976	3.037	3.174	3.237	3.626	3.483	3.023	2.765	3.203	2.960	2.414	2.890
F ⁻	b.d.l.	0.112	0.088	0.094	0.257	0.104	0.125	0.105	0.100	b.d.l.	0.087	0.104
O ²⁻	25.024	24.852	24.738	24.670	24.117	24.413	24.852	25.130	24.697	25.040	25.499	25.006
Bvn (mol.%)	55.8	44.8	40.4	37.8	2.2	21.7	45.1	54.9	38.1	50.9	75.0	53.0
An. No. Sample Type	13 Vla PH	14 Vla PH	15 Drza Brl	16 Drzb D	17 Draa Brl	18 Vez D	19 Vez D	20 Nyza Brl	21 Nyza Brl	22 Maa Brl	23 Mab D	24 Mae D
Wt.%												
P ₂ O ₅	b.d.l.	b.d.l.	0.09	b.d.l.	b.d.l.	b.d.l.	0.09	b.d.l.	b.d.l.	0.07	0.08	b.d.l.
SiO ₂	58.31	58.58	57.06	58.52	58.85	60.39	60.08	59.19	58.79	57.89	59.01	60.16
Al ₂ O ₃	10.99	7.18	7.08	4.70	5.41	1.37	2.35	2.65	6.04	5.18	6.17	3.97
BeO*	5.38	7.32	7.50	8.94	8.47	10.70	10.25	9.70	7.94	8.46	7.90	9.25
MnO	b.d.l.	b.d.l.	b.d.l.	0.10	0.06	b.d.l.	b.d.l.	b.d.l.	b.d.l.	b.d.l.	b.d.l.	b.d.l.
CaO	23.83	23.39	24.32	25.02	24.71	24.61	24.63	24.66	24.27	24.34	23.79	24.93
Na ₂ O	0.18	0.51	0.16	0.16	0.15	0.49	0.53	b.d.l.	0.10	0.19	0.39	0.10
H ₂ O*	1.99	2.65	2.57	3.05	2.94	3.90	3.72	3.25	2.75	2.89	2.78	3.21
F	b.d.l.	0.28	0.14	0.24	0.20	0.09	0.09	0.49	0.27	0.27	0.35	0.27
O=F	0.00	-0.12	-0.06	-0.10	-0.08	-0.04	-0.04	-0.21	-0.11	-0.12	-0.15	-0.12
Total	100.68	99.79	98.86	100.63	100.71	101.51	101.70	99.73	100.05	99.19	100.32	101.78
Atoms per formula unit												
P ⁵⁺	b.d.l.	b.d.l.	0.011	b.d.l.	b.d.l.	b.d.l.	0.011	b.d.l.	b.d.l.	0.009	0.010	b.d.l.
Si ⁴⁺	9.004	8.998	8.883	8.884	8.936	8.950	8.920	8.987	8.993	8.918	8.991	8.983
^{iva} Al ³⁺	0.000	0.002	0.106	0.116	0.064	0.050	0.069	0.013	0.007	0.074	0.000	0.017
Subtotal	9.004	9.000	9.000	9.000	9.000	9.000	9.000	9.000	9.000	9.000	9.001	9.000
^{ivb} Al ³⁺	2.000	1.298	1.194	0.726	0.903	0.189	0.342	0.461	1.082	0.868	1.108	0.681
Be ²⁺	1.996	2.702	2.806	3.262	3.089	3.811	3.658	3.538	2.919	3.132	2.891	3.319
Mn ²⁺	b.d.l.	b.d.l.	b.d.l.	0.012	0.008	b.d.l.	b.d.l.	b.d.l.	b.d.l.	b.d.l.	b.d.l.	b.d.l.
Subtotal	3.996	4.000	4.000	4.000	4.000	4.000	4.000	4.000	4.000	4.000	3.999	4.000
Ca ²⁺	3.943	3.850	4.057	4.070	4.021	3.909	3.918	4.012	3.978	4.017	3.884	3.989
Na ⁺	0.054	0.152	0.049	0.046	0.044	0.142	0.151	b.d.l.	0.030	0.056	0.115	0.028
Subtotal	3.997	4.002	4.106	4.116	4.064	4.050	4.069	4.012	4.007	4.074	3.999	4.017
H ⁺	2.052	2.716	2.668	3.088	2.980	3.860	3.689	3.292	2.810	2.973	2.826	3.200
F ⁻	b.d.l.	0.136	0.069	0.116	0.097	0.042	0.040	0.235	0.131	0.133	0.169	0.129
O ²⁻	25.948	25.148	25.263	24.795	24.924	24.098	24.271	24.473	25.060	24.894	25.005	24.670
Bvn (mol.%)	100.0	64.9	59.7	36.3	45.2	9.5	17.1	23.1	54.1	43.4	55.4	34.1

Sample types: Brl, Hlv, Phk – proximal in pseudomorphs after beryl, helvine and phenakite, respectively; D – distal; PH – pocket hydrothermal.
b.d.l. – below detection limit, * – calculated from stoichiometry.

(2.00–0.67 Al apfu). Evident zoning is developed in the Alpine-type vein from Schinderhübel I (Fig. 3e) where mono-mineral aggregates of bohseite in quartz are Al-poor (≥ 0.58

apfu) whereas bavenite–bohseite associated with epidote and pumpellyite in central part of the veinlet is Al enriched (≤ 1.25 apfu). Also, distal bavenite–bohseite associated with muscovite

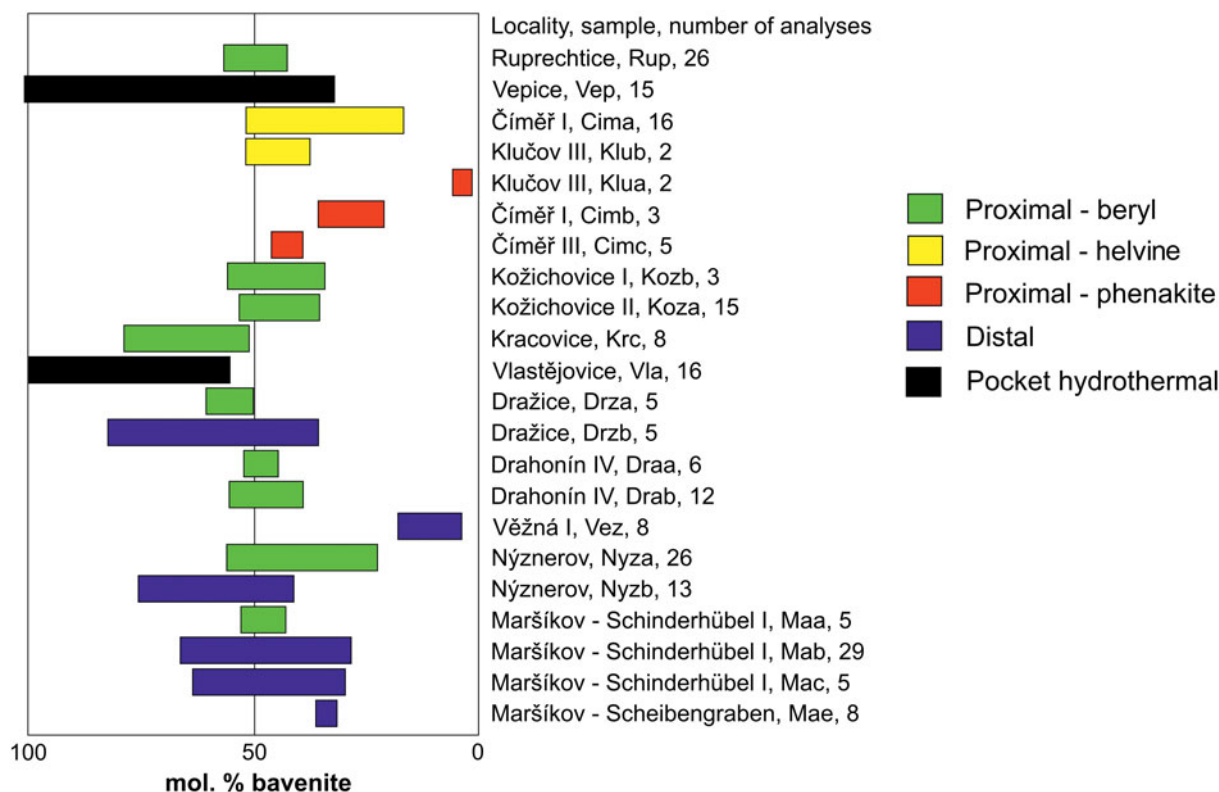


Figure 4. Ranges of bavenite–bohseite compositions in individual samples.

from the Maršíkov Schinderhübel I pegmatite is heterogeneous (1.31–0.58 Al apfu) as well as distal bavenite–bohseite from Dražice (1.69–0.96 Al apfu).

Raman spectroscopy

Bavenite–bohseite, and some associated primary and secondary minerals, were identified using the Raman spectroscopy (unoriented). Secondary phenakite was not observed in the assemblages of secondary minerals for any of the samples investigated whereas bertrandite was identified in several samples (see Table 4). Here, we present a newly-acquired spectrum of bohseite. Raman spectroscopy was also used to identify minerals of bavenite–bohseite series and to identify eventual structure variations based on compositional changes. For this investigation, three representative samples were selected: a bavenite-rich sample from Vlastějovice; bavenite/bohseite from Ruprechtice; and a bohseite-rich sample from Věžná I (Fig. 4). All samples have similar bavenite spectra (Lafuente *et al.*, 2015) with slight peak shifts and differences; only the bohseite spectrum is contaminated with some kind of fluorescence.

Discussion

Composition of bavenite–bohseite

We focused primarily on the variations in Al content on the basis of a large set of EPMA data (Table 5, Fig 4). The individual paragenetic types have been discussed separately to reveal differences between them and to demonstrate the role of a Be precursor combined with variations in composition of hydrothermal fluids that facilitated crystallisation of bavenite–bohseite with a diverse origin

(proximal *versus* distal). We have also tried to compare the composition of the individual paragenetic types of bavenite–bohseite with the published data. However, this task was very difficult due to frequent absence of information regarding textural and paragenetic positions of the bavenite–bohseite samples analysed with respect to potential or evident primary Be mineral precursors (see De Michele, 1967 and references therein). Furthermore, significant differences in the compositions among bavenite–bohseite samples from the same locality presented by the individual authors (e.g. Fleischer and Switzer, 1953; Lussier and Hawthorne, 2011) as well as the absence of analysed minor elements (Fe, Mn, P, Na and F) in most published papers partly obscure such discussion.

The samples of hydrothermal bavenite and bavenite–bohseite from miarolitic pockets are typically rich in Al (2.00–0.67 apfu) and very heterogeneous (Fig. 4, Table 5). This paragenetic type differs significantly from the other recognised types of bavenite–bohseite in having high Al contents, however only two examined samples are not sufficient for a comprehensive discussion. Similar miarolitic bavenite to bavenite–bohseite was studied at several localities, e.g. Baveno, Italy (Lussier and Hawthorne, 2011), Cape Granite Suite, South Africa (Scheepers *et al.*, 2017) and Bustarviejo, Madrid, Spain (Garcia-Guinea *et al.*, 2005). Their compositions yielded high Al in the Cape Granite (1.82–2.01 apfu) but high variability in Baveno (0.62 and 1.41 apfu; Fleischer and Switzer, 1953; Lussier and Hawthorne, 2011). In the alkaline pegmatite from Mont Saint-Hilaire, Canada miarolitic bohseite is Al-poor (0.53 apfu Al; Lussier and Hawthorne, 2011).

Proximal and distal bavenite–bohseite yielded almost the same variations in the concentrations of Al (1.56–0.05 apfu and 1.69–0.09 apfu, respectively; Fig. 4). Bohseite with very low to moderate Al is typical in pseudomorphs after Al-free Be-precursors

(phenakite and helvine–danalite), whereas bavenite–bohseite after beryl in LCT pegmatites has higher Al (Fig. 4). The proximal bavenite–bohseite after beryl from the NYF pegmatites Kožichovice I and II with moderate Al (Fig. 4) reflects lower content of Al in primary Mg,Fe-enriched beryl (Table 2) compared to the LCT pegmatites with very low Mg and Fe given above. At the Dražice and Schinderhübel I pegmatites, distal bavenite exhibits higher variation (1.69–0.84 apfu and 1.25–0.66 apfu, respectively) than the proximal one (1.47–1.10 apfu and 1.04–0.94 apfu, respectively). Accordingly, proximal bavenite–bohseite reflects mainly the composition of the precursor whereas compositions of distal bavenite–bohseite are more heterogeneous and could mirror variability in activities of Al and Be in fluids. In addition, associated secondary minerals (e.g. bertrandite) in proximal bavenite–bohseite or Be-free Al-bearing phases (K-feldspar, muscovite, epidote, pumpellyite and zeolites) in both distal and proximal bavenite–bohseite may have controlled concentration of Al in bavenite–bohseite.

Moderate concentrations of Na were found in the distal bohseite from Věžná I (≤ 0.71 Na₂O; ≤ 0.20 apfu Na) and they are similar to other bavenite–bohseite (Lussier and Hawthorne, 2011; Szeleg *et al.*, 2017). Elevated concentrations of Fe and Mn in proximal bavenite–bohseite from the Čiměř I pegmatite (Table 5) reflect the composition of the precursor – helvine–danalite (Fig. 3), whereas elevated Fe but no Mn in the proximal bavenite–bohseite after beryl from Kožichovice I mirrors elevated Fe in primary Mn-free beryl (Table 2). Moderate contents of Mg in primary beryl and its absence in the relevant secondary proximal and distal bavenite–bohseite (Fig. 5) as well as in the distal bavenite–bohseite associated with epidote + pumpellyite at the Schinderhübel I pegmatite imply that Mg is very probably not compatible with the crystal structures of bavenite and bohseite. This is also supported by the concentrations of Mg below the detection limit (~ 400 ppm) in all analysed samples.

The variability of two most common minor elements Na and F in the individual types of bavenite–bohseite are shown in Fig. 5. Both samples of primary hydrothermal miarolitic bavenite–bohseite differ; bavenite–bohseite from Vepice IV is enriched in F (Fig. 5a,b) whereas bavenite from Vlastějovice is F-poor. The distal type typically contains slightly higher concentrations of Na compared to the proximal type, whereas concentrations of F are similar. The distal type also yields a positive correlation for F/Al whereas primary bavenite–bohseite from Vepice IV has a negative F/Al correlation (Fig. 5c). In summary, differences in the concentrations of Na and F among the individual types of bavenite–bohseite are minor. Because almost all published data included no determination of Fe and Mn and in most cases no F and Na, except for Lussier and Hawthorne (2011) and Szeleg *et al.* (2017), a comprehensive comparison with the other analytical data published previously is not desirable.

Raman spectroscopy of bavenite–bohseite

Assignment of bands in the Raman spectra is theoretically possible. Tentative assignments of Raman bands was done based on similarities with different silicate minerals or minerals with beryllate tetrahedra. Raman spectra were compared with cyclosilicates, both single chain and multiple chain inosilicates and framework silicates. A certain resemblance with the spectra of framework silicates was observed, and our results for the bavenite–bohseite series seem to be in agreement with work by

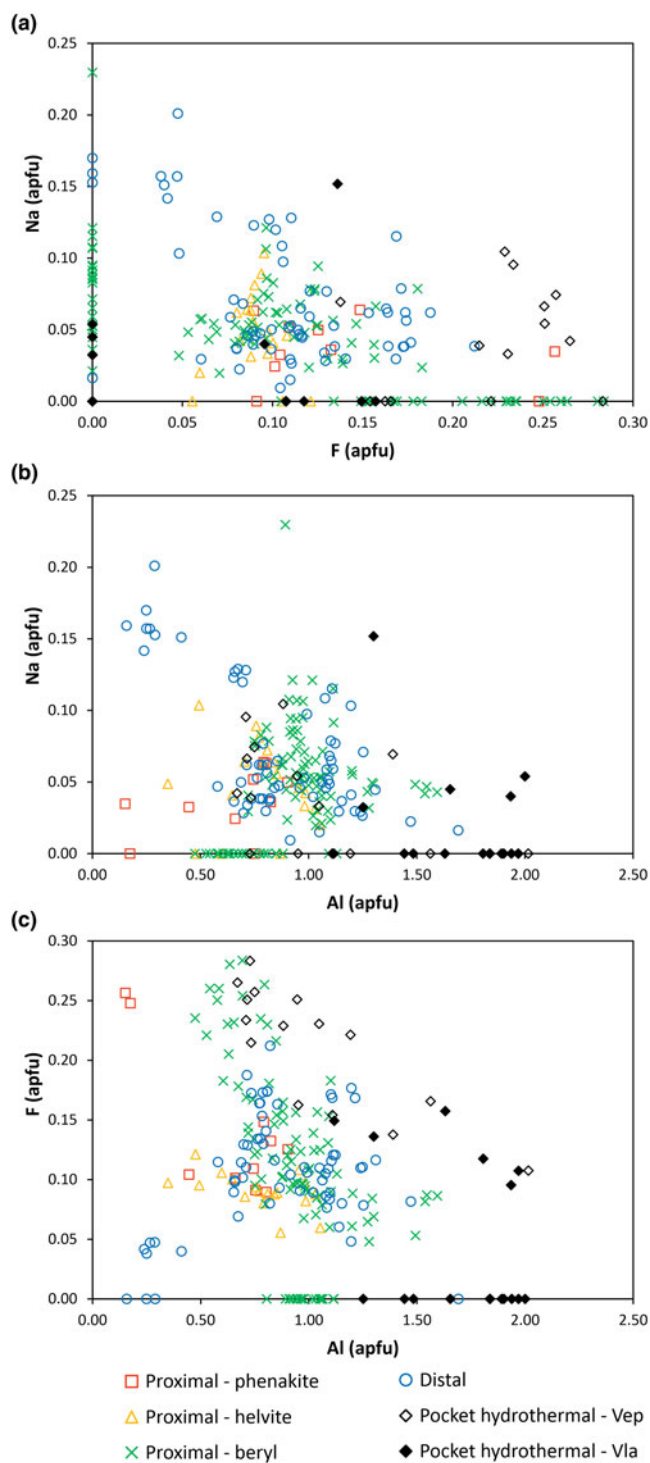


Figure 5. Compositional variation diagrams of bavenite–bohseite. (a) F/Na; (b) Na/Al; and (c) F/Al.

Cannillo *et al.* (1966) and later Lussier and Hawthorne (2011) who list the minerals of this series as framework silicates.

Spectra in the range of 100–300 cm⁻¹ could be related to lattice vibrations and the area including Raman bands from 300 cm⁻¹ to 600 cm⁻¹ presumably belongs to SiO₄ modes combined with Ca–O bonds – their shifts being due to OH⁻ vibration and translation (Fig. 6a). Part of the spectrum from 650 cm⁻¹ to 760 cm⁻¹ probably involves the contribution of the relative motion of the

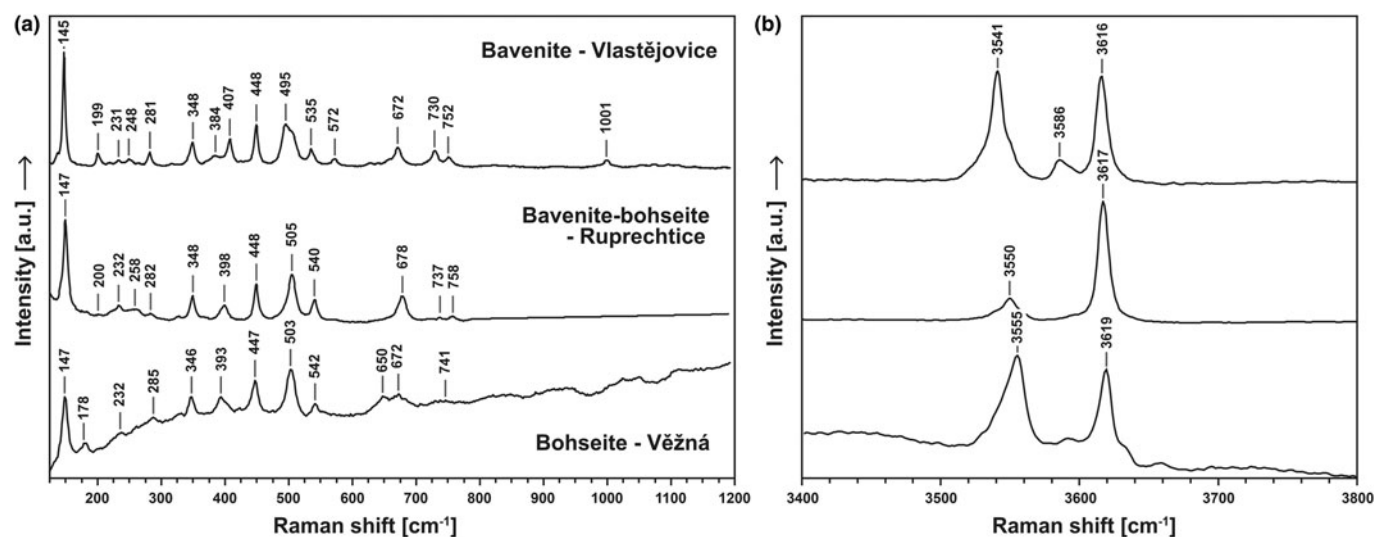


Figure 6. Raman spectra of bavenite, 1:1 bavenite–bohseite and bohseite. (a) spectral range 100–1200 cm^{-1} and (b) spectral range 3400–3800 cm^{-1} .

tetrahedrally coordinated Be atoms in adjacent chain links $\text{BeO}_4\text{-SiO}_4\text{-BeO}_4$ (Prencipe *et al.*, 2006; Szeleş *et al.*, 2017).

Comparison of the Raman spectra in the OH^- region with their calculated contents unambiguously shows that the overall composition has a strong influence on the mutual arrangement of these OH^- vibrational modes (similar correlation has been observed in tourmalines – see Huy *et al.*, 2011). The Raman spectra obtained in the range of 3400–3800 cm^{-1} is given in Fig. 6b. The vibration at $\sim 3617 \text{ cm}^{-1}$ is relatively consistent, whereas the modes lower than 3555 cm^{-1} vary in accord with the relative proportions of the bavenite and bohseite components. On the basis of this observation, we can assume that with increasing bohseite component, the distance between the OH^- vibrational modes decreases. This result can then be linked to the observations from the crystallographic study of bohseite by Szeleş *et al.* (2017).

Mineral assemblages of bavenite–bohseite

(1) Hydrothermal bavenite and bavenite–bohseite from miarolitic pockets occur in the Vlastějovice and Vepice IV pegmatites where a potential primary Be-precursor is absent (Table 4). The absence of a primary Be mineral in these pegmatites implies that the concentration of Be in melt was not sufficiently high to precipitate beryl (>60 ppm Be in low- T granitic melt: London and Evensen, 2002) or other primary Be mineral. Residual fluids enriched in Be facilitated the origin of bavenite–bohseite as a primary hydrothermal Be mineral in a miarolitic pocket; elevated concentration of Ca in these residual fluids is crucial. The investigated mineral assemblages of hydrothermal bavenite–bohseite are rather similar to other occurrences in miarolitic pockets from intragranitic pegmatites (e.g. Baveno, Italy – Fleischer and Switzer, 1953; Strzegom, Poland – Janeczka, 1986; Cape Granite Suite, South Africa – Scheepers *et al.*, 2017; Bustarviejo, Madrid, Spain – Garcia-Guinea *et al.*, 2005), where additional Ca-rich minerals (epidote, fluorite, calcite, prehnite, stilbite, laumontite and axinite) and chlorite are typically associated; however, epidote, fluorite, prehnite, chlorite and zeolites are absent at the examined localities of miarolitic hydrothermal bavenite–bohseite. Only the Vlastějovice pegmatite is evidently LCT affiliated (Novák *et al.*, 2013) whereas all other pegmatites with

miarolitic hydrothermal bavenite–bohseite discussed above are typically NYF affiliated. High activity of Ca in the fluids essential for the origin of hydrothermal bavenite–bohseite has two distinct sources in the examined pegmatites: residual fluids derived from pegmatite in intragranitic NYF pegmatites (e.g. Třebíč Pluton) and pre-emplacment contamination of pegmatite melt from host Fe-skarn at the LCT elbaite pegmatite Vlastějovice (Novák *et al.*, 2013).

(2) The proximal assemblages after primary Be minerals (Table 4) include several distinct paragenetic and textural types. Total to almost complete bavenite–bohseite pseudomorphs with rare relics of primary Be precursor (beryl) are common at most localities (Ruprechtice, Kracovice, Dražice, Drahonín IV and Schinderhübel I); bavenite–bohseite is commonly associated with bertrandite and locally with K-feldspar, muscovite-illite, gismondine-Ca, analcime, laumontite and/or scolecite (Table 4, Fig. 2,3). Veinlets with bavenite–bohseite as the sole product of replacement of primary phenakite and helvine–danalite are typical in pegmatites of the Třebíč Pluton (Zachař *et al.*, 2020). However, more complex secondary assemblages after beryl were also found in this region: bavenite–bohseite + beryl + bazzite + smectite (Kořichovice II), bohseite + milarite (Číměř I, Kořichovice II), bohseite + bazzite (Kořichovice II), bavenite + clinozoisite (Kořichovice II, Číměř I), bohseite + axinite (Číměř I; Novák and Filip, 2010; Zachař *et al.*, 2020). Bohseite dominates in pseudomorphs after Al-free minerals phenakite and helvine–danalite, and its textures are similar to the proximal bavenite–bohseite after beryl (Fig. 3d). In the Třebíč Pluton, secondary Be minerals occur almost exclusively within pseudomorphs, except for rare bavenite–bohseite on the surface of beryl crystals (Fig. 2d). The total absence of typical secondary distal Be minerals on brittle tectonic fractures and fissures is a distinctive feature of the Třebíč pegmatite region.

(3) The distal bavenite–bohseite is variable in morphology and mineral assemblages. Most brittle fractures and fissures continue to their host rock and are evidently related to tectonism. Externally derived fluids running through fractures were responsible for the alteration of beryl (or other primary Be mineral) and facilitated formation of distal bavenite–bohseite. Bavenite–bohseite in radial aggregates or as fine-grained chalk-like coatings apparently not associated with further secondary minerals is the

most common paragenetic type (Table 4). At the Dražice pegmatite, abundant distal bavenite–bohseite typically occurs with K-feldspar. At the Schinderhübel I pegmatite, further minerals occur in a close association with distal bavenite–bohseite: muscovite + albite + quartz or epidote + pumpellyite + quartz (Table 4, Fig. 3e). At the Dražice and Schinderhübel I pegmatites, where both proximal and distal bavenite were identified, proximal bavenite–bohseite has a simpler mineral assemblage compared to the distal bavenite–bohseite which also has more variable composition (Fig. 4). Moreover, distal bavenite–bohseite is not associated with bertrandite even at the localities where abundant bertrandite occurs with the proximal bavenite–bohseite (Table 4).

It is difficult to compare the types of bavenite–bohseite occurrences described in the present study with published reports because the information provided on paragenetic and textural relationships of bavenite–bohseite in these reports was not sufficient to distinguish primary hydrothermal miarolitic, or secondary proximal and distal types (e.g. Fleischer and Switzer, 1953; Janeczek, 1986; Lussier and Hawthorne, 2011). Nevertheless, the mineral assemblages observed of proximal and distal bavenite–bohseite are rather different from those described by Černý (1968, 2002). In particular, the widespread proximal assemblage bavenite + bertrandite at almost all localities of LCT pegmatites (Table 4) is remarkable and does not fit with the published observations. According to Černý (2002), bertrandite is typically associated with muscovite and less commonly with K-feldspar; phenakite and euclase are the only associated secondary Be minerals with bavenite–bohseite. Abundance of K-feldspar and higher variability of the mineral assemblages in distal bavenite–bohseite from the examined pegmatites suggest that bavenite–bohseite and/or bertrandite may be stable over a wider range of *P–T–X* conditions (see the Discussion below).

Mineral reactions involving bavenite–bohseite

Actual mineral reactions generating bavenite–bohseite from the primary Be-rich precursors (beryl, phenakite and helvine–danalite) are difficult to formulate due to variable compositions of the primary beryl and mainly secondary bavenite–bohseite, in addition to locally complex textural relations in the secondary mineral assemblages. Several idealised reactions involving beryl as a primary Be precursor are presented in Table 6 (#1–5), using the ideal compositions of all involved Be minerals and/or the composition bavenite–bohseite = 1:1.

Reactions 1 and 2 illustrate two theoretical settings where Si + Al or only Si are entirely fixed in secondary minerals. Alteration following reaction 1 was observed at the Dražice pegmatite, where released Be and Al facilitated the development of a wide halo of abundant distal bavenite–bohseite on fractures around the altered

beryl crystals; the potential excess of Al was incorporated in K-feldspar commonly associated with bavenite–bohseite (Table 4). The assemblage bavenite + bertrandite in pseudomorphs after beryl at Kracovice (Fig. 3f) shows that the modified reaction 3 is close to the real situation at this locality where distal secondary Be minerals are probably absent or very rare (Němec, 1990). The modified reactions 3 and 4 illustrate that the proportions of bavenite or bohseite components in the mineral may vary significantly. The more Al is contained in bavenite–bohseite the more modal bertrandite may be present in the assemblage if we assume that no Be was released from the system. At the localities with the assemblage proximal bavenite–bohseite + bertrandite after beryl, higher contents of Al in bavenite–bohseite are typical (e.g. Kracovice; Fig. 2f). More complex proximal assemblages observed in the Třebíč pegmatites including also secondary beryl and bazzite do not change the reaction 4 significantly because beryl is at both sides of the reaction. Scandium in secondary bazzite was supplied by primary Sc-enriched beryl (Novák and Filip, 2010). Secondary milarite $\text{Ca}_2\text{K}(\text{Be}_2\text{Al})\text{Si}_{12}\text{O}_{30}(\text{H}_2\text{O})$ requires elevated K, which is commonly present in fluids manifested at other localities by abundant K-feldspar, muscovite, and/or muscovite–illite (Table 4).

Reactions 6–8 in Table 6, involving Al-free primary Be minerals – phenakite and helvine–danalite were created with bohseite s.s. and bavenite/bohseite = 1/1 as alteration products.

The mineral assemblages observed are mostly simple and contain only bohseite after phenakite with no Be being released during the reaction 6. This is a good fit with the pseudomorphs after phenakite in pegmatites of the Třebíč Pluton where bohseite is a sole proximal secondary Be mineral and distal secondary Be minerals are absent (Table 4, Fig. 2b). In the helvine–danalite pseudomorphs, bohseite is associated locally with rare secondary danalite II (Table 4); however, it modifies reaction 8 only slightly (helvine–danalite is on both sides of the reaction) and low f_{O_2} is necessary for the formation of secondary danalite II (Barton and Young, 2002). However, the occurrence of jarosite in pseudomorphs after phenakite described by Zachař (2021) demonstrates that the released S and M^{2+} cations facilitated origin of a secondary sulfate mineral at high f_{O_2} . These contrasting assemblages (helvine–danalite *versus* jarosite) manifest high variability of f_{O_2} in the fluids which facilitated origin of secondary proximal bohseite at the Třebíč pegmatites.

Significant input of Ca and H_2O are necessary in all the reactions and, in addition, input of Si and locally Al is required for some reactions. The beryl-, phenakite- and helvine–danalite-involving reactions differ in the abundance of Al which facilitates origin of Al-rich bavenite and further distal Al-bearing secondary minerals (K-feldspar and muscovite). They are common mostly in distal secondary assemblages after beryl in the LCT pegmatites (Dražice, Schinderhübel I;

Table 6. Idealised reactions (1–5) involving beryl as a primary Be precursor using the ideal compositions of all involved Be minerals and/or the composition bavenite–bohseite = 1:1; and reactions (6–8) involving Al-free primary Be minerals – phenakite and helvine–danalite created with bohseite s.s. and bavenite/bohseite = 1/1 as alteration products.

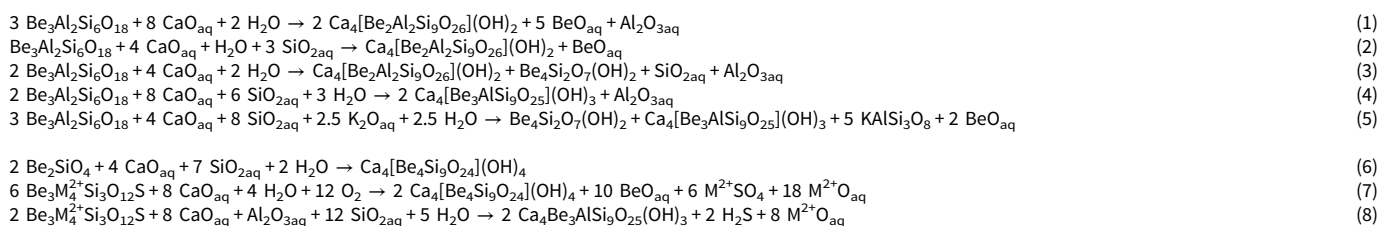


Table 3), however are mostly absent or rare in the proximal assemblages.

P-T-X conditions of bavenite–bohseite origin

Because Ca is an essential constituent of bavenite and bohseite, these minerals have not been considered in experimental and thermodynamic studies performed in the BASH and Na–BASH systems (e.g. Barton, 1986; Barton and Young, 2002; Markl, 2001; Wang and Li, 2020). Consequently, the *P-T-X* conditions may be estimated only from the textural relations and associated minerals as was done by Scheepers *et al.* (2017) for a miarolitic pocket at the Cape Granite, South Africa. The *P-T* stability of the associated minerals (stilbite–Ca), fluid-inclusion study, and mainly the chlorite geothermometry suggest $T = 210\text{--}320^\circ\text{C}$ and $P < 2$ kbar. At the Vlastějovice pegmatite, the absence of Mg but elevated contents of Sn in coeval axinite–(Mn) indicate that the miarolitic pocket system was closed to the host rock (Fe–skarn) during crystallisation of pocket minerals. The crystallisation of hydrothermal bavenite at rather high $T \approx 300\text{--}400^\circ\text{C}$ (London, 2008) is reasonable and it fits very well with the crystallisation *T* of axinite–(Mn) in miarolitic pockets in the pegmatitic gem-tourmaline deposit, Malkhan, Transbaikalia at $285\text{--}415^\circ\text{C}$ (Zagorsky *et al.*, 2016).

Together with bavenite–bohseite as the dominant proximal mineral, bertrandite is widespread in the investigated pseudomorphs after beryl (Table 4). It is stable at $T < 240^\circ\text{C}$, $P = 100$ MPa and low activity of Al (Fig. 7; Barton, 1986; Barton and Young, 2002). Formation of bavenite–bohseite at $T \approx 200\text{--}300^\circ\text{C}$ is indicated by the presence of coeval bertrandite and zeolites in the proximal bavenite–bohseite assemblages. On the one hand, these zeolites could have crystallised at temperatures as high as 310°C : analcime at $T < 300^\circ\text{C}$ (Neuhoff *et al.*, 2004),

scolecite at $T < 310^\circ\text{C}$ (e.g. Weisenberger, 2009) and gismondine–Ca at $T = 110\text{--}250^\circ\text{C}$ (Ghobarkar and Schäf, 1999; Chung *et al.*, 2002). On the other hand, these zeolites may have crystallised at a much lower temperature, $T \approx 100\text{--}150^\circ\text{C}$ (e.g. Weisenberger and Bucher, 2010). Nevertheless, the presence of epidote + pumpellyite in the assemblage with distal coeval bavenite–bohseite (Fig. 4e) suggests crystallisation at $T > \sim 200\text{--}250^\circ\text{C}$ (Frey and Robinson, 2009; Liou *et al.*, 1983, 1985). Accordingly, the temperature of crystallisation of bavenite–bohseite associated with bertrandite + K-feldspar and with epidote + pumpellyite was estimated at $T \approx 200\text{--}300^\circ\text{C}$ and these values are similar to the data of Scheepers *et al.* (2017). In summary, bavenite–bohseite crystallised over a temperature range of 400 to $\sim 100\text{--}150^\circ\text{C}$ estimated from its coeval crystallisation with zeolites (Weisenberger, 2009) and other minerals (Frey and Robinson, 2009; Liou *et al.*, 1983, 1985).

The pressure of bavenite–bohseite crystallisation may be estimated from its geological position and mineral assemblages. Hydrothermal bavenite–bohseite from miarolitic pockets is a primary mineral which crystallised in the very early stage of the hydrothermal process of pegmatite consolidation. At the Vlastějovice pegmatite, the pressure of crystallisation in the miarolitic pocket was similar to the pressure during emplacement of rare-element pegmatite at lithostatic $P < \sim 200\text{--}300$ MPa (Ackerman *et al.*, 2007). Relatively high pressure is indicated for the distal bavenite–bohseite coeval with the assemblage epidote + pumpellyite in the Alpine-type veinlet cutting the quartz core of the Maršíkov Schinderhübel I pegmatite (Table 4, Fig. 3e) where $P > \sim 150\text{--}200$ MPa is a reasonable estimate based on its association with pumpellyite (Frey and Robinson 2009). In contrast, at some localities secondary proximal bavenite–bohseite is associated with zeolites (Table 4) which typically crystallised at low $P < \sim 50\text{--}100$ MPa or even

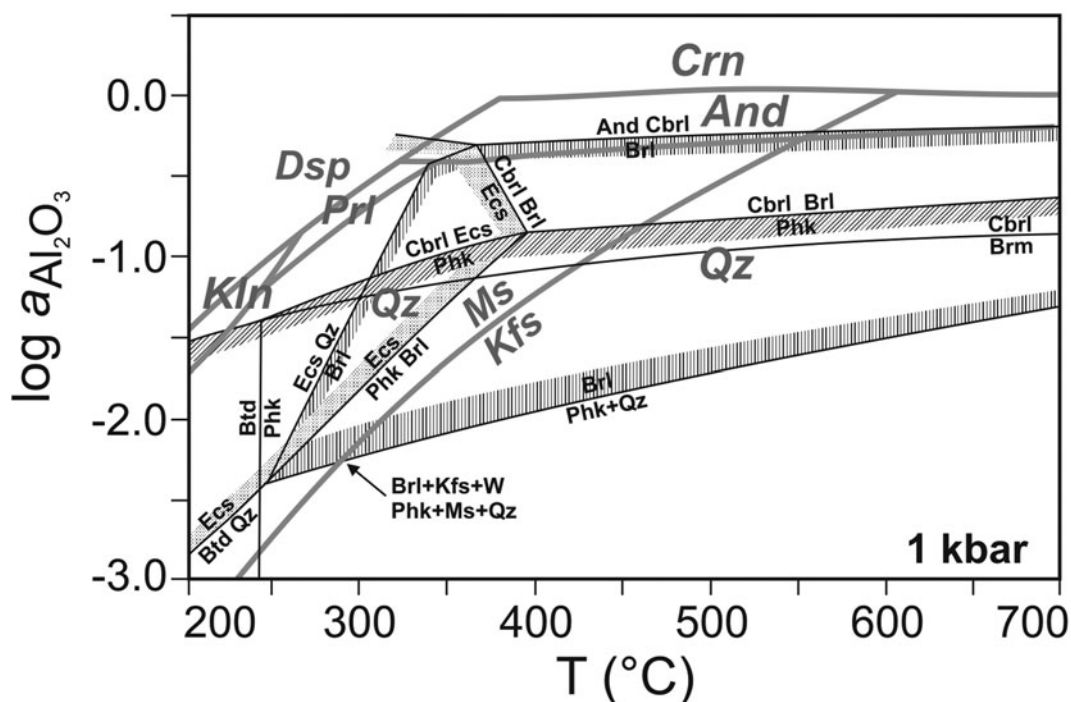


Figure 7. Beryllium minerals stability as a function of temperature and the activity of alumina (modified from Barton and Young, 2002). Note the small stability field of the assemblage bertrandite + K-feldspar.

lower $P < \sim 15\text{--}20$ MPa (Chipera and Apps, 2001; Weisenberger, 2009; Weisenberger and Bucher, 2010) as is indicated by the occurrence of scolecite with the proximal bavenite–bohseite at the Drahonín IV pegmatite. Hydrostatic pressure (see Palinkaš *et al.*, 2014) at $P < 50$ MPa is assumed for fissure-filling secondary distal, and probable for part of secondary proximal, bavenite–bohseite, respectively.

Bertrandite is considered to form in acidic to neutral conditions by Černý (2002); however, associated smectite, adularia, axinite and zeolites (analcime, scolecite, laumontite and gismondine-Ca), are common in the proximal bavenite–bohseite assemblages (Table 4), and indicate instead alkaline to neutral conditions (Hedenquist *et al.*, 2000; Weisenberger and Bucher, 2010). Moreover, the secondary assemblages epididymite + bertrandite + K-feldspar + muscovite (Novák *et al.*, 1991) and bertrandite + K-feldspar + magnesio-arfvedsonite (Čopjaková *et al.*, 2021), both after beryl from the Věžná I pegmatite, are additional evidence that the stability of bertrandite might be considered as being of moderately alkaline conditions. The results of our study suggest that the stability fields of the relevant Be minerals in $P\text{--}T\text{--}X$ diagrams require further experimental study (e.g. Wang and Li, 2020) as well as thorough study of their mineral assemblages.

Geochemical signature of fluids producing bavenite–bohseite

Secondary minerals generated by hydrothermal alteration of primary minerals are indicators of the composition of hydrothermal fluids in distinct stages of subsolidus evolution of granitic pegmatites. Together with typical cations and anions (see e.g. London, 2008) Ca and Mg also were commonly detected in subsolidus alteration products. Magnesium evidently has an external origin in most cases (e.g. Novák *et al.*, 1999, 2012, 2017b; Čopjaková *et al.*, 2021) but an external or internal source of Ca is a matter of discussion (e.g. Teertstra *et al.*, 1999; Martin and de Vito, 2014; Novák *et al.*, 2013, 2017b; Pieczka *et al.*, 2019; Zachař *et al.*, 2020; Gadas *et al.*, 2022), and obviously might differ in the individual pegmatites.

The mineral assemblages of hydrothermal bavenite and bavenite–bohseite from miarolitic pockets suggest elevated activities of the same cations (Be, Ca, Si, Al, Mn and Fe) but distinct differences in volatiles in residual fluids ($\text{H}_2\text{O} + \text{B}$) and ($\text{H}_2\text{O} + \text{CO}_2 + \text{S}$) at the Vlastějovice and Vepice IV pegmatites, respectively, as indicated by their mineral assemblages. Moreover, the occurrence of Sn-enriched axinite–(Mn) from Vlastějovice suggests a more complex composition of residual fluids manifested in a higher degree of fractionation of this Li-bearing pegmatite (Novák *et al.*, 2013). The mineral assemblages as well as composition of proximal bavenite–bohseite (Table 4) demonstrates high activity of Ca in fluids but locally also elevated activities of K (K-feldspar; Kracovice), Na (analcime; Drahonín IV), and Fe + Mn + B + S (axinite and danalite; Číměř I). In contrast, Si, Fe, Mn and S were derived from a primary Be-precursor (helvine–danalite) in the latter case. The assemblages of distal bavenite–bohseite illustrate the dominance of Ca in fluids together with locally elevated activities of K (K-feldspar, muscovite, muscovite–illite), Na (albite), Mg + Fe (epidote, pumpellyite), and Si (recrystallisation of quartz). Participation of external fluids as sources for Ca, Mg and other cations, derived from the host amphibole gneiss is evident in the distal assemblage bavenite–bohseite + epidote + pumpellyite + quartz from the Maršíkov Schinderhübel I pegmatite. Close spatial relations of bavenite to

epidote veins cutting the host pegmatite has also been described from Cava Grignaschi, Italy (De Michele, 1967). The albitisation of early-formed plagioclase from host amphibole gneiss is very likely to be the source of Ca (cf. Martin and de Vito 2014, Weisenberger and Bucher, 2011) and is supported by elevated Sr contents of epidote from the Maršíkov, Schinderhübel I pegmatite that was probably derived during albitisation of rock-forming plagioclase from the host metabasite. At the Věžná I pegmatite (Table 1), H_2O - and Ca-rich, CO_2 -poor serpentinite-derived fluids are an important source of Ca (e.g. Palandri and Reed, 2004; Chavagnac *et al.*, 2013; Evans *et al.*, 2013; Čopjaková *et al.*, 2021) together with Mg. At NYF pegmatites of the Třebíč Pluton, residual fluids are the most probable source of Ca, manifested not only by abundant proximal secondary bavenite–bohseite but also other late proximal secondary Ca-rich minerals including abundant titanite after ilmenite (Škoda *et al.*, 2006; Zachař and Novák, 2013), microlite + fersmite + kristiansenite after columbite (Výravský *et al.*, 2019), and high Ca contents in both solidus and subsolidus tourmalines (Novák *et al.*, 2011).

A high activity of Ca in residual fluids is essential for the origin of hydrothermal bavenite–bohseite in miarolitic pockets. This might be explained by the total absence of apatite in the pegmatite which is a typical sink for Ca in distinct stages of pegmatite evolution (London, 2008; Martin and de Vito, 2014). All examined localities, except for the Nýznerov, Věžná I and Scheibengraben pegmatites, contain very rare apatite or it is absent (Table 4). Bavenite–bohseite occurs in a variety of NYF and LCT granitic pegmatites (Table 1); however, it is absent at some LCT pegmatites from the region of the Bohemian Massif where rich assemblages of secondary Be minerals were observed. The beryl–columbite pegmatites from the Písek region, Moldanubicum (e.g. Černý *et al.*, 2007; Škoda *et al.*, 2011; Švecová *et al.*, 2016) are typical examples with very abundant late fluorapatite in miarolitic pockets, and abundant secondary bertrandite, typically proximal in pockets after dissolved beryl. This is commonly associated with secondary muscovite together with rather rare proximal milarite, secondary beryl, phenakite and danalite (Novák and Cempírek, 2010). Notwithstanding the detailed scientific study of these pegmatites, including Be minerals (Vrba, 1895; Sejkora *et al.*, 1998; Novák and Cempírek, 2010) bavenite–bohseite has not been identified to date (pers. comm. J. Cicha). An absence of Ca-enriched external fluids together with residual fluids depleted in Ca due to sequestration of abundant late fluorapatite at these pegmatites did not allow formation of bavenite–bohseite and demonstrates the importance of apatite abundance in the pegmatite for the availability of Ca in both residual and external fluids.

Conclusions and summary

Bavenite–bohseite was recognised as the most abundant secondary Be mineral in the NYF, mixed and LCT pegmatites of the Bohemian Massif. Three distinct textural and paragenetic types were recognised. (1) Rare primary hydrothermal bavenite–bohseite from miarolitic pockets; (2) proximal secondary bavenite–bohseite in pseudomorphs after primary Be minerals (beryl, helvine–danalite and phenakite); and (3) distal secondary bavenite–bohseite mostly in brittle tectonic fractures and fissures within the host pegmatite. Hydrothermal bavenite–bohseite from miarolitic pockets is typically the only Be mineral in the pegmatite. In contrast, secondary proximal bavenite–bohseite is commonly associated with other secondary Be minerals after beryl – bertrandite,

milarite, beryl, danalite and bazzite (see Table 4). We recommend using the terms primary hydrothermal, proximal or distal secondary mineral in the descriptions of bavenite–bohseite and other secondary Be minerals together with a detailed study of actual paragenetic position of secondary Be minerals and their relations to their potential primary Be precursors.

The individual types of bavenite–bohseite differ in their Al contents (Fig. 4). Hydrothermal bavenite to bavenite–bohseite from miarolitic pockets is Al-rich (2.00–0.67 Al apfu); proximal bavenite–bohseite gave variable Al with low contents (1.02–0.05 Al apfu) in pseudomorphs after phenakite and helvine–danalite, and higher contents (1.56–0.69 Al apfu) in pseudomorphs after beryl; distal bavenite–bohseite is the most variable (1.63–0.09 Al apfu) (Table 5, Fig. 4). Proximal bavenite–bohseite reflects mainly the composition of the Be mineral precursor whereas compositions of distal bavenite–bohseite are more heterogeneous and mirror the variability of hydrothermal fluids. The petrogenetic family of the host pegmatite (LCT, NYF) is important only for the composition of primary hydrothermal bavenite–bohseite in pockets. Thus, bavenite is typical for LCT and bohseite for NYF pegmatites, respectively.

The bavenite–bohseite solid solutions range in compositions from $Bv_{100}Bhs_0$ to $Bv_{22}Bhs_{98}$; with compositions close to $Bv_{50}Bhs_{50}$ being the most common (Fig. 4). Only traces of Na, F, Fe, Mn and P were detected. Raman spectra in the range of 3400–3800 cm^{-1} vary chiefly in the vibrational modes lower than 3555 cm^{-1} in accord with the relative proportions of the bavenite and bohseite components (Fig. 6b). With these modes, the composition of the samples examined can be recognised quite reliably.

Calcium is an essential element together with Be, Si and Al, which were mostly released from primary Be mineral precursors. Presuming an external source for Ca is reasonable in the case of the pegmatite contaminated from a serpentinite host, which supplied Mg and Ca. Similarly, the metamorphic overprint of the pegmatites demonstrated by Alpine-type hydrothermal fissure fillings with epidote ± pumpellyite, albite, and bavenite–bohseite supplied external Ca. For intragranitic NYF pegmatites, residual fluids are the most probable source of Ca as well as in the pegmatite cutting an Fe skarn where external Ca contamination of pegmatite melt proceeded during pre-emplacment and/or post-emplacment stages (Novák, 2013; Novák et al., 2013) before the crystallisation of bavenite and bavenite–bohseite in pockets.

Primary hydrothermal bavenite from miarolitic pockets crystallised at rather high $T \approx 300$ – $400^\circ C$, whereas distal Al-poor bohseite is a very late fracture-hosted mineral formed at rather low $T \approx 100$ – $150^\circ C$. The PT stability fields of the associated minerals allow us to propose that bavenite–bohseite is stable over a range of pressures from ~ 15 to ~ 150 MPa. The mineral assemblages and position of bavenite–bohseite in pegmatite evolution (miarolitic, hydrothermal proximal and distal) indicate that bavenite-dominant compositions may have crystallised at higher temperatures relative to bohseite-dominant ones. However, this must be confirmed by further studies.

Acknowledgements. The authors thank the Principal Editor Roger Mitchell, and reviewers E. Szeleg and P. Uher for constructive criticism that significantly improved the manuscript. This research was supported by OP RDE [grant number CZ.02.1.01/0.0/0.0/16_026/0008459 (Geobarr) from the ERDF] for MN and RŠ. The research was financially supported by the Ministry of

Culture of the Czech Republic (long-term project DKRVO 2019-2023/1.II.e; National Museum, 00023272; to ZD and LV).

Competing interests. The authors declare none.

References

- Ackerman L., Zachariáš J. and Pudilová M. (2007) P–T and fluid evolution of barren and lithium pegmatites from Vlastějovice, Bohemian Massif, Czech Republic. *International Journal of Earth Sciences*, **96**, 623–638.
- Barton M. (1986) Phase equilibria and thermodynamic properties of minerals in the BeO – Al_2O_3 – SiO_2 – H_2O (BASH) system, with petrologic applications. *American Mineralogist*, **71**, 277–300.
- Barton M. and Young S. (2002) Non-pegmatitic deposits of beryllium: mineralogy, geology, phase equilibria and origin. Pp. 591–691 in: *Beryllium – Mineralogy, Petrology and Geochemistry* (E.S. Grew, editor). Reviews in Mineralogy and Geochemistry, 50. Mineralogical Society of America, Washington DC.
- Burt D. (1978) Multisystems analysis of beryllium mineral stabilities: the system BeO – Al_2O_3 – SiO_2 – H_2O . *American Mineralogist*, **63**, 664–676.
- Cannillo E., Coda A. and Fagani G. (1966) The crystal structure of bavenite. *Acta Crystallographica*, **20**, 301–309.
- Černý P. (1960) Milarite and wellsite from Věžná. *Práce Brněnské Základny Československé Akademie Věd*, **32**, 1–16 [in Czech].
- Černý P. (1963) Epididymite and milarite – alteration products of beryl from Věžná, Czechoslovakia. *Mineralogical Magazine*, **33**, 450–457.
- Černý P. (1965) *Mineralogy of two Pegmatites from the Věžná Serpentinite*. CSc thesis, Geological Institute of the ČSAV Prague, Prague, Czechoslovakia [in Czech].
- Černý P. (1968) Berylliumwandlungen in Pegmatiten - Verlauf und Produkte. *Neues Jahrbuch für Mineralogie, Abhandlungen*, **108**, 166–180.
- Černý P. (2002) Mineralogy of beryllium in granitic pegmatites. Pp. 405–444 in: *Beryllium – Mineralogy, Petrology and Geochemistry* (E.S. Grew, editor). Reviews in Mineralogy and Geochemistry, 50. Mineralogical Society of America, Washington DC.
- Černý P. and Ercit T.S. (2005) The classification of granitic pegmatites revisited. *The Canadian Mineralogist*, **43**, 2005–2026.
- Černý P., Novák M. and Chapman R. (1992) Effects of sillimanite-grade metamorphism and shearing on Nb,Ta-oxide minerals in granitic pegmatites: Maršákov, northern Moravia, Czechoslovakia. *The Canadian Mineralogist*, **30**, 699–718.
- Černý P., Novák M., Chapman R. and Ferreira K.J. (2007) Subsolidus behavior of niobian rutile from the Písek region, Czech Republic: a model for exsolution in W- and Fe^{2+} >> Fe^{3+} -rich phases. *Journal of Geosciences*, **52**, 143–159.
- Chavagnac V., Monnin Ch., Ceuleneer G., Boulart C. and Hoareau G. (2013) Characterization of hyperalkaline fluids produced by low-temperature serpentinization of mantle peridotites in the Oman and Ligurian ophiolites. *Geochemistry Geophysics Geosystems*, **14**, 2496–2522.
- Chipera S.J. and Apps J.A. (2001) Geochemical stability of natural zeolites. Pp. 117–161 in: *Natural Zeolites: Occurrences, Properties, Applications* (D.L. Bish and D.W. Ming, editors). Reviews in Mineralogy and Geochemistry, 45. Mineralogical Society of America, Washington DC.
- Chládek Š., Uher P. and Novák M. (2020) Compositional and textural variations of columbite-group minerals from beryl-columbite pegmatites, the Maršákov District, Bohemian Massif, Czech Republic: magmatic versus hydrothermal evolution. *The Canadian Mineralogist*, **58**, 767–783.
- Chládek Š., Uher P., Novák M., Bačík P. and Opletal T. (2021) Microlite-group minerals: tracers of complex post-magmatic evolution in beryl-columbite granitic pegmatites, Maršákov District, Bohemian Massif, Czech Republic. *Mineralogical Magazine*, **85**, 725–743.
- Chung S.H., Chen Y.L., Lin I.C. and Li L. (2002) Syntheses of zeolites of the gismondine group. *Western Pacific Earth Sciences*, **2**, 331–346.
- Čopjaková R., Škoda R., Vašinová-Galiová M., Novák M. and Cempírek J. (2015) Scandium- and REE-rich tourmaline replaced by Sc-rich REE-bearing

- epidote-group mineral from the mixed (NYF + LCT) Kracovice pegmatite (Moldanubian Zone, Czech Republic). *American Mineralogist*, **100**, 1434–1451.
- Čopjaková R., Prokop J., Novák M., Losos Z. and Gadas P. (2021) Hydrothermal alterations of tourmaline from pegmatitic rocks enclosed in serpentinites; multistage processes with distinct fluid sources. *Lithos*, **380**, 105823.
- De Michele V. (1967) Bavenite nella pegmatite di Cava Grignaschi (Val d'Ossola). *Atti della Società Italiana di Scienze Naturali e del Museo Civico di Storia Naturale di Milano*, **106**, 171–179.
- Dolníček Z., Nepejchal M. and Novák M. (2020) Minerals of the bavenite-bohseite series from the Schinderhübel I pegmatite in Maršíkov (Silesicum, Czech Republic). *Bulletin Mineralogie Petrologie*, **28**, 353–358 [in Czech with English summary].
- Dosbaba M. and Novák M. (2012) Quartz replacement by “kerolite” in graphic quartz-feldspar intergrowths from the Věžná I pegmatite, Czech Republic; A complex desilicification process related to episyenitization. *The Canadian Mineralogist*, **50**, 1609–1622.
- Evans B.W., Hattori K. and Barronet A. (2013) Serpentinites: What, why and when. *Elements*, **9**, 99–106.
- Fleischer M. and Switzer G. (1953) The bavenite problem. *American Mineralogist*, **38**, 988–993.
- Franz G. and Morteani G. (1984) The formation of chrysoberyl in metamorphosed pegmatites. *Journal of Petrology*, **25**, 27–52.
- Franz G. and Morteani G. (2002) Be-minerals synthesis, stability, and occurrence in metamorphic rocks. Pp. 551–598 in: *Beryllium – Mineralogy, Petrology and Geochemistry* (E.S. Grew, editor). Reviews in Mineralogy and Geochemistry, 50. Mineralogical Society of America, Washington DC.
- Frey M. and Robinson D. (editors) (2009) *Low-Grade Metamorphism*. John Wiley & Sons, New Jersey, USA.
- Friis H., Makovicky E., Weller M.T. and Lemée-Cailleau M.-H. (2010) Bohseite, IMA 2010-026. CNMNC Newsletter, 2010, *Mineralogical Magazine*, **74**, 797–800.
- Gadas P., Novák M., Galiová M.V., Szuszkiewicz A., Pieczka A., Haifler J. and Cempírek J. (2020) Secondary beryl in cordierite/sekaninaite pseudomorphs from granitic pegmatites – a monitor of elevated content of beryllium in the precursor. *The Canadian Mineralogist*, **58**, 785–802.
- Gadas P., Novák M., Vašinová Galiová M.V. and Pezzotta F. (2022) Chemical composition of tourmalines from granitic pegmatite and its exocontact at Manjaka, Sahatany Valley, Madagascar; EPMA and LA-ICP-MS study. *Journal of Geosciences*, in print
- García-Guinea J., Correcher V., Quejido A., LaIglesia A. and Can N. (2005) The role of rare earth elements and Mn²⁺ point defects on the luminescence of bavenite. *Talanta*, **65**, 54–61.
- Ghobarkar H. and Schäfer O. (1999) Synthesis of gismondine-type zeolites by the hydrothermal method. *Materials Research Bulletin*, **34**, 517–525.
- Grew E.S. (2002) Beryllium in metamorphic environments (emphasis on aluminous compositions). Pp. 487–549 in: *Beryllium – Mineralogy, Petrology and Geochemistry* (E.S. Grew, editor). Reviews in Mineralogy and Geochemistry, 50. Mineralogical Society of America, Washington DC.
- Grew E.S. and Hazen R.M. (2014) Beryllium mineral evolution. *American Mineralogist*, **99**, 999–1021.
- Grew E.S., Yates M.G., Shearer C.K., Hagerty J.J., Sheraton J.W. and Sandiford M. (2006) Beryllium and other trace elements in paragneisses and anatectic veins of the ultrahigh-temperature Napier Complex, Enderby Land, East Antarctica: The role of sapphirine. *Journal of Petrology*, **47**, 859–882.
- Grice J.D., Rowe R., Poirier G., Pratt A. and Francis J. (2009) Bussyite-(Ce), a new beryllium silicate mineral species from Mont Saint-Hilaire, Quebec. *The Canadian Mineralogist*, **47**, 193–204.
- Hålenius U., Hatert F., Pasero M. and Mills S.J. (2015) IMA Commission on New Minerals, Nomenclature and Classification (CNMNC) Newsletter 24. New minerals and nomenclature modifications approved in 2015. *Mineralogical Magazine*, **79**, 247–251.
- Hawthorne F.C. and Huminicki D.M.C. (2002) The crystal chemistry of beryllium. Pp. 333–403 in: *Beryllium – Mineralogy, Petrology and Geochemistry* (E.S. Grew, editor). Reviews in Mineralogy and Geochemistry, 50. Mineralogical Society of America, Washington DC.
- Hedenquist J.W., Arribas A.R. and Gonzalez-Urien E. (2000) Exploration for epithermal gold deposits. *SEG Reviews*, **13**, 245–277.
- Hsu L.C. (1983) Some phase relationships in the system BeO–Al₂O₃–SiO₂–H₂O with comments on effects of HF. *Geological Society China Memoire*, **5**, 33–46.
- Huy L.H., Nguyen M.T.H., Chen B.-X., Ming V.N. and Yang S.I. (2011) Raman spectroscopy study of various types of tourmalines. *Journal of Raman Spectroscopy*, **42**, 1442–1446.
- Janeček J. (1986) Chemistry, optics, and crystal growth of milarite from Strzegom, Poland. *Mineralogical Magazine*, **50**, 271–277.
- Lafuente B., Downs R., Yang H. and Stone N. (2015) 1. The power of databases: The RRUFF project. Pp. 1–30 in: *Highlights in Mineralogical Crystallography* (T. Armbruster and R. Danisi, editors). De Gruyter (O), Berlin, München, Boston.
- Liou J.G., Kim H.S. and Maruyama S. (1983) Prehnite–epidote equilibria and their petrologic applications. *Journal of Petrology*, **24**, 321–342.
- Liou J.G., Maruyama S. and Cho M. (1985) Phase equilibria and mineral parageneses of metabasites in low-grade metamorphism. *Mineralogical Magazine*, **49**, 321–333.
- London D. (2008) Pegmatites. *The Canadian Mineralogist, Special Publication*, **10**, 1–347.
- London D. and Evensen M.J. (2002) Beryllium in silicic magmas and the origin of beryl-bearing pegmatites. Pp. 445–486 in: *Beryllium – Mineralogy, Petrology and Geochemistry* (E.S. Grew, editor). Reviews in Mineralogy and Geochemistry, 50. Mineralogical Society of America, Washington DC.
- Lussier A.J. and Hawthorne F.C. (2011) Short-range constraints on chemical and structural variations in bavenite. *Mineralogical Magazine*, **75**, 213–239.
- Manning D.A.C., Putthapiban P. and Suensilpong S. (1983) An occurrence of bavenite, Ca₄Be₂Al₂(SiO₃)₉·xH₂O, in Thailand. *Mineralogical Magazine*, **47**, 87–89.
- Markl G. (2001) Stability of Na-Be minerals in late-magmatic fluids of the Ilímaussaq alkaline complex, South Greenland. *Geology of Greenland Survey Bulletin*, **190**, 145–158.
- Markl G. and Schumacher J. (1997) Beryl stability in local hydrothermal and chemical environments in a mineralized granite. *American Mineralogist*, **82**, 195–203.
- Martin R.F. and De Vito C.D. (2014) The late-stage miniflood of Ca in granitic pegmatites: an open-system acid-reflux model involving plagioclase in the exocontact. *The Canadian Mineralogist*, **52**, 165–181.
- Němec D. (1990) Neues zur Mineralogie eines Hambergit-führenden Pegmatitgangs von Kracovice (bei Třebíč, Westmorava, ČSFR). *Zeitschrift Geologische Wissenschaften*, **18**, 1105–1115.
- Neuhoff P.S., Hovis G.L., Balassone G. and Stebbins J.F. (2004) Thermodynamic properties of analcime solid solutions. *American Journal of Science*, **304**, 21–66.
- Novák M. (2013) Contamination processes in complex granitic pegmatites. *PEG 2013: The 6th International Symposium on Granitic Pegmatites*, **2013**, 100–103.
- Novák M. and Cempírek J. (2010) Granitic pegmatites and mineralogical museums in the Czech Republic. IMA2010. Field trip guide CZ2. *Acta Mineralogica-Petrographica, Field guide series*, **6**, 1–56.
- Novák M. and Filip J. (2010) Unusual (Na,Mg)-enriched beryl and its breakdown products (beryl II, bazzite, bavenite) from euxenite-type NYF pegmatite related to the orogenic ultrapotassic Třebíč Pluton, Czech Republic. *The Canadian Mineralogist*, **48**, 615–628.
- Novák M., Korbelt P. and Odehnal F. (1991) Pseudomorphs of bertrandite and epididymite after beryl from Věžná, Western Moravia, Czechoslovakia. *Neues Jahrbuch für Mineralogie, Monatshefte*, **1991**, 473–480.
- Novák M., Burns P.C. and Morgan G.B. (1998) Fluorine variation in hambergite from granitic pegmatites. *The Canadian Mineralogist*, **36**, 441–446.
- Novák M., Selway J., Černý P., Hawthorne F.C. and Ottolini L. (1999) Tourmaline of the elbaite-dravite series from an elbaite-subtype pegmatite at Bližná, southern Bohemia, Czech Republic. *European Journal of Mineralogy*, **11**, 557–568.
- Novák M., Černý P. and Uher P. (2003) Extreme variation and apparent reversal of Nb-Ta fractionation in columbite-group minerals from the Scheibengraben beryl-columbite pegmatite, Maršíkov, Czech Republic. *European Journal of Mineralogy*, **15**, 565–574.
- Novák M., Škoda R., Filip J., Macek I. and Vaculovič T. (2011) Compositional trends in tourmaline from intragranitic NYF pegmatites of the Třebíč Pluton, Czech Republic: an electron microprobe, Mössbauer and LA-ICP-MS study. *The Canadian Mineralogist*, **49**, 359–380.

- Novák M., Škoda R., Gadas P., Krmíček L. and Černý P. (2012) Contrasting origins of the mixed (NYF+LCT) signature in granitic pegmatites, with examples from the Moldanubian Zone, Czech Republic. *The Canadian Mineralogist*, **50**, 1077–1094.
- Novák M., Kadlec T. and Gadas P. (2013) Geological position, mineral assemblages and contamination of granitic pegmatites in the Moldanubian Zone, Czech Republic; examples from the Vlastějovice region. *Journal of Geosciences*, **58**, 21–47.
- Novák M., Čopjaková R., Dosebaba M., Galiová M.V., Všianský D. and Staněk J. (2015a) Two paragenetic types of cookeite from the Dolní Bory-Hatě pegmatites, Moldanubian Zone, Czech Republic: Proximal and distal alteration products of Li-bearing sekaninaite. *The Canadian Mineralogist*, **53**, 1035–1048.
- Novák M., Gadas P., Cempírek J., Škoda R., Breiter K., Kadlec T., Loun J. and Toman J. (2015b) B1 Granitic pegmatites of the Moldanubian Zone, Czech Republic. *PEG 2015: 7th International Symposium on Granitic Pegmatites, Field trip guidebook*, **2015**, 23–72.
- Novák M., Cícha J., Čopjaková R., Škoda R. and Galiová M.V. (2017a) Milarite-group minerals from the NYF pegmatite Velká skála, Písek district, Czech Republic: sole carriers of Be from the magmatic to hydrothermal stage. *European Journal of Mineralogy*, **29**, 755–766.
- Novák M., Prokop J., Losos Z. and Macek I. (2017b) Tourmaline, an indicator of external Mg-contamination of granitic pegmatites from host serpentinite; examples from the Moldanubian Zone, Czech Republic. *Mineralogy and Petrology*, **111**, 625–641.
- Palandri J.L. and Reed M. (2004) Geochemical models of metasomatism in ultramafic systems: Serpentinization, rodingitization, and sea floor carbonate chimney precipitation. *Geochimica et Cosmochimica Acta*, **68**, 1115–1133.
- Palinkaš S.S., Wegner R., Čobič A., Palinkaš L.A., Barreto S.D.B., Váczi T. and Bermanec, V. (2014) The role of magmatic and hydrothermal processes in the evolution of Be-bearing pegmatites: Evidence from beryl and its breakdown products. *American Mineralogist*, **99**, 424–432.
- Pieczka A., Szuskiewicz A., Szeleg E. and Nejbert K. (2019) Calcium minerals and late stage metasomatism in the Julianna pegmatitic system, the Góry Sowie Block, SW Poland. *PEG 2019, Contributions to the 9th International Symposium*, **2019**, 56–58.
- Pouchou J.L. and Pichoir F. (1985) “PAP” (phi-rho-z) procedure for improved quantitative microanalysis. Pp. 104–106 in: *Microbeam Analysis* (J.T. Armstrong, editor). San Francisco Press, San Francisco, USA.
- Prencipe M., Noel Y., Civalleri B., Roetti C. and Dovesi R. (2006) Quantum-mechanical calculation of the vibrational spectrum of beryl (Al₄Be₆Si₁₂O₃₆) at the Γ point. *Physics and Chemistry of Minerals*, **33**, 519–532.
- Rao C., Wang R.C. and Hu H. (2011) Paragenetic assemblages of beryllium silicates and phosphates from the Nanping no. 31 granitic pegmatite dyke, Fujian province, southeastern China. *The Canadian Mineralogist*, **49**, 1175–1187.
- Scheepers R., O’Brien R.D. and Schoch A.E. (2017) An occurrence of bavenite in the Cape Granite Suite, southwestern Cape Province, South Africa, and its implication on the formation of the host pegmatite. *South African Journal of Geology*, **120**, 223–230.
- Sejkora J., Litochleb J., Exnar P., Černý P. and Čech F. (1998) Some physical-chemical data for pink beryl (morganite) from Písek pegmatites. *Bulletin Czech Geological Survey*, **73**, 347–350 [in Czech with English summary].
- Škoda R., Novák M. and Houzar S. (2006) Granitic NYF pegmatites of the Třebíč Pluton. *Acta Musei Moraviae, Scientiae Geologicae*, **91**, 129–176 [in Czech with English summary].
- Škoda R., Novák M. and Cícha J. (2011) Uranium–niobium-rich alteration products after “písekite”, an intimate mixture of Y, REE, Nb, Ta, Ti-oxide minerals from the Obrázek I pegmatite, Písek, Czech Republic. *Journal of Geosciences*, **56**, 317–325.
- Sojka A. (1969) *Mineralogical and Textural/Paragenetic Relations in Pegmatites from Ore-Deposit Olší*. Unpublished Ms thesis, Masaryk University, Brno, Czech Republic [in Czech].
- Švecová E., Čopjaková R., Losos Z., Škoda R., Nasdala L. and Cícha J. (2016) Multi-stage evolution of xenotime–(Y) from Písek pegmatites, Czech Republic: an electron probe micro-analysis and Raman spectroscopy study. *Mineralogy and Petrology*, **110**, 747–765.
- Szeleg E., Zuzens B., Hawthorne F.C., Pieczka A., Szuskiewicz A., Turniak K., Nejbert K., Ilnicki S.S., Friis H., Makovicky E., Weller M.T. and Lemée-Cailleau M.-H. (2017) Bohseite, ideally Ca₄Be₄Si₉O₂₄(OH)₄, from the Piława Górna quarry, the Góry Sowie Block, SW Poland. *Mineralogical Magazine*, **81**, 35–46.
- Teertstra D.K., Černý P. and Ottolini L. (1999) Stranger in paradise: liddicoatite from the High Grade Dike pegmatite, southeastern Manitoba, Canada. *European Journal of Mineralogy*, **11**, 227–236.
- Toman J. and Novák M. (2018) Textural relations and chemical composition of minerals from a pollucite + harmotome + chabazite nodule in the Věžná I pegmatite, Czech Republic. *The Canadian Mineralogist*, **56**, 375–392.
- Toman J. and Novák M. (2020) Beryl-columbite pegmatite Věžná I. *Acta Musei Moraviae, Scientiae Geologicae*, **107**, 3–42 [in Czech with English summary].
- Uher P., Ozdín D., Bačík P., Števko M., Ondrejka M., Rybnikova O., Chládek Š., Fridrichová J., Pršek J. and Puškelová L. (2022) Phenakite and bertrandite: products of post-magmatic alteration of beryl in granitic pegmatites (Tatric Superunit, Western Carpathians, Slovakia). *Mineralogical Magazine*, **86**, 715–729.
- Vrba K. (1895) Über Beryllium-Mineralen aus der Umgebung von Písek. *Bulletin International Academia Science L’imperial Francois Joseph I*, **2**, 1–16.
- Výravský J., Škoda R. and Novák M. (2019) Kristiansenite, thortveitite and ScNbO₄: Products of Ca-metasomatism of Sc-enriched columbite-(Mn) from NYF pegmatite Kožichovice II, Czech Republic. *PEG2017 8th International Symposium on Granitic Pegmatites*, **2017**, 169–172.
- Wang X. and Li J. (2020) In situ observations of the transition between beryl and phenakite in aqueous solutions using a hydrothermal diamond-anvil cell. *The Canadian Mineralogist*, **58**, 803–814.
- Warr L.N. (2021) IMA–CNMNC approved mineral symbols. *Mineralogical Magazine*, **85**, 291–320.
- Weisenberger T. (2009) *Zeolites in Fissures of Crystalline Basement Rocks*. Unpublished Ph.D. thesis, Universität Freiburg, Freiburg, Germany.
- Weisenberger T. and Bucher K. (2010) Zeolites in fissures of granites and gneisses of the Central Alps. *Journal of Metamorphic Geology*, **28**, 825–847.
- Weisenberger, T. and Bucher K. (2011) Mass transfer and porosity evolution during low temperature water–rock interaction in gneisses of the Simano nappe: Arvigo, Val Calanca, Swiss Alps. *Contributions to Mineralogy and Petrology*, **162**, 61–81.
- Wood S.A. (1992) Theoretical prediction of speciation and solubility of beryllium in hydrothermal solution to 300° C at saturated vapor pressure: Application to bertrandite/phenakite deposits. *Ore Geology Reviews*, **7**, 249–278.
- Zachář A. (2021) *Granitic Pegmatites of the Třebíč Pluton; Distribution, Geological Position and Mineralogy*. Unpublished Ph.D. thesis, Masaryk University, Brno, Czech Republic [in Czech with English summary].
- Zachář A. and Novák M. (2013) Granitic NYF pegmatites in the Velké Meziříčí region, Třebíč Pluton, western Moravia (Czech Republic). *Acta Musei Moraviae, Scientiae Geologicae*, **98**, 83–100 [in Czech with English summary].
- Zachář A., Novák M. and Škoda R. (2020) Beryllium minerals as monitors of geochemical evolution from magmatic to hydrothermal stage; examples from NYF pegmatites of the Třebíč Pluton, Czech Republic. *Journal of Geosciences*, **65**, 153–172.
- Zagorsky V.Y., Peretyazhko I.S. and Dmitrieva A.S. (2016) Axinite-(Mn) from miarolitic granitic pegmatites of the Malkhan gem-tourmaline deposit (Transbaikalia, Russia): composition, paragenesis and conditions of formation. *European Journal of Mineralogy*, **28**, 811–824.